

UNCLASSIFIED

AD 4 5 0 6 2 7

DEFENSE DOCUMENTATION CENTER

FOR

SCIENTIFIC AND TECHNICAL INFORMATION

CAMERON STATION ALEXANDRIA, VIRGINIA



UNCLASSIFIED

NOTICE: When government or other drawings, specifications or other data are used for any purpose other than in connection with a definitely related government procurement operation, the U. S. Government thereby incurs no responsibility, nor any obligation whatsoever; and the fact that the Government may have formulated, furnished, or in any way supplied the said drawings, specifications, or other data is not to be regarded by implication or otherwise as in any manner licensing the holder or any other person or corporation, or conveying any rights or permission to manufacture, use or sell any patented invention that may in any way be related thereto.

450627

TR 64-052.7

450627

CATALOGED BY DDC

AS AD NO. \_\_\_\_\_

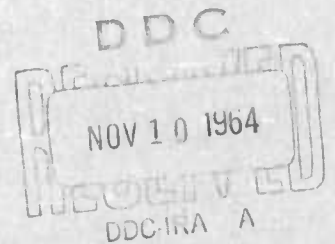
**CHELATE LASERS  
ANNUAL TECHNICAL SUMMARY REPORT**

Contract No. NONr-4134(00)  
ARPA Order No. 306-62

1 October 1963 - 30 September 1964

Issued: 30 October 1964

A. Lempicki  
H. Samelson  
C. Brecher



**GENERAL TELEPHONE & ELECTRONICS LABORATORIES  
INCORPORATED**

**BAYSIDE LABORATORIES, BAYSIDE, NEW YORK**



TR 64-052.7

CHELATE LASERS

ANNUAL TECHNICAL SUMMARY REPORT

Contract No. NONr-4134(00)

ARPA Order No. 306-62

1 October 1963 - 30 September 1964

Issued: 30 October 1964

A. Lempicki  
H. Samelson  
C. Brecher

This research is part of Project DEFENDER under the joint sponsorship of the Advanced Research Projects Agency, The Office of Naval Research and the Department of Defense.

Reproduction in whole or in part is permitted for any purpose of the United States Government.

General Telephone & Electronics Laboratories Inc.  
Bayside, New York

## TABLE OF CONTENTS

	<u>Page</u>
1. INTRODUCTION	1
2. SUMMARY OF PREVIOUS WORK	1
3. PROPERTIES OF THE MATERIAL	3
3.1 Solution Chemistry of the Chelates	3
3.2 Spectroscopic Properties of the Chelates	6
3.3 Solvent and Salt Effects	13
3.4 Effects on Laser Action	18
4. PROPERTIES OF THE LASER	23
4.1 General Considerations and Experimental Arrangement	23
4.2 Apparatus	28
4.3 Output Power	29
4.4 Output Beam Characteristics	31
4.5 Quality of the Optical Cavity	37
5. CONCLUSIONS	40
PAPERS PUBLISHED	41
REFERENCES	42

## LIST OF ILLUSTRATIONS

	<u>Page</u>
Fig. 1. Emission spectra of europium dibenzoylmethide in alcohol solution.	8
Fig. 2. Emission spectra of europium benzoylacetate in alcohol solution.	10
Fig. 3. Emission spectra of europium benzoyltrifluoroacetate in alcohol solution.	12
Fig. 4. Emission spectra of europium dibenzoylmethide in DMFA solution.	14
Fig. 5. Emission spectra of europium benzoylacetate in DMFA solution.	15
Fig. 6. Emission spectra of europium benzoyltrifluoroacetate in DMFA solution.	16
Fig. 7. Fluorescence emission spectrum of an 0.01M solution of $\text{Eu}(\text{BTF})_4\text{P}$ in (a) acetonitrile (b) dimethylformamide at $25^\circ\text{C}$ .	17
Fig. 8. Fluorescence emission spectra of (a) 0.01M $\text{EuB}_4\text{P}$ in alcohol at $-150^\circ\text{C}$ ; (b) spectrum of solid adduct at $-150^\circ\text{C}$ .	19
Fig. 9. Fluorescence emission spectra of $\text{EuB}_4\text{P}$ in dimethylformamide.	20
Fig. 10. Emission spectra of 0.01 M $\text{EuB}_4\text{P}$ in alcohol at $-150^\circ\text{C}$ with various input energies to the flash tube and different concentrations of sodium acetate.	24
Fig. 11. Energy level diagram of a europium chelate.	26
Fig. 12. Cells used in laser experiments (a) 1-mm bore, (b) 4-mm bore.	30
Fig. 13. Relaxation oscillation (random spikes) obtained from $\text{EuB}_4\text{P}$ in 1-mm cavity.	32
Fig. 14. Fabry-Perot interferograms of the output of $\text{EuB}_4\text{P}$ in alcohol solution.	33

LIST OF ILLUSTRATIONS (Cont'd.)

	<u>Page</u>
Fig. 15(a). Near field pattern of laser emission from 1-mm cell.	34
Fig. 15(b). Intermediate field pattern.	35
Fig. 16. Regular relaxation pattern (limit cycle) characteristic of $\text{EuB}_4\text{P}$ in large (4 mm) cells.	36
Fig. 17. Dependence of laser threshold of $\text{EuB}_4\text{P}$ in alcohol solution on concentration.	38
Fig. 18. Output energy of the 0.10-cm cell versus percent transmission of front mirror at twice threshold.	39

## 1. INTRODUCTION

The research on chelate lasers at the General Telephone & Electronics Laboratories has been organized along two general lines. The first is an investigation of the properties of the materials in terms of the requirements for laser action. The second is a study of the characteristics of the chelate laser itself. The resultant information is essential for a full appreciation of the potential of chelate laser systems.

Originally, the only chelate capable of exhibiting laser action was europium tetrakis benzoylacetate, and the temperature of operation was below  $160^{\circ}\text{K}$ . As our understanding of these materials increased, we have been able to add to the number of chelates that can serve as laser materials, chemically shift the frequency of one chelate laser system by about  $60\text{ cm}^{-1}$ , and increase the operating temperature, in one case as high as  $300^{\circ}\text{K}$ . The results of this research have been published in a series of papers<sup>1-7</sup> in which more detailed information can be found. These results indicate that the achievement of room-temperature laser action in a circulating fluid medium is not only practicable but, at this point, awaits only the development on suitable technological services.

## 2. SUMMARY OF PREVIOUS WORK

The material in this section summarizes studies previously reported in the Semiannual Technical Summary Report of 1963 and in references 1 and 2. These publications presented a detailed analysis of the spectroscopy of europium benzoylacetate ( $\text{EuB}_4\text{P}$ ) and of the kinetics of fluorescence from the laser viewpoint.

A detailed analysis of the emission spectra of  $\text{EuB}_4\text{P}$  in solution and in the solid enables us to partially construct the energy level diagram of the europium ion. The fluorescent emission levels are the  $^5\text{D}_0$  and  $^5\text{D}_1$  upper states, and most of the emission occurs from the former. All of the states of the  $^7\text{F}$  multiplet serve as terminal states for the emissive transition, but the principal emission is to one of the levels of the  $^7\text{F}_2$  state, some  $900\text{ cm}^{-1}$  above ground. Thus at low temperatures, the terminal state is essentially empty, and even at room temperature the population of this one level is less than 1.5 percent of the ground state. The europium chelate can therefore be considered a four level system.

In the chelates the energy is absorbed in the organic component of the molecule, and according to the model of Weissman<sup>8</sup> and Crosby,<sup>9</sup> it relaxes from the excited singlet to the triplet and is then transferred to the europium ion. On the basis of this model the kinetics of fluorescence can be analyzed in terms of specific rate constants or transition probabilities for each of the steps in the process. The results of this analysis indicate that for typical rate constants usually reported for intersystem crossing and energy transfer, there should be no impediment to achieving laser action. Under some conditions, however, a "bottleneck" could arise in the triplet state. At this point it is possible for the energy to be diverted to a lower triplet level and then appear as long-lived phosphorescence. If this happens, it will be almost impossible to attain sufficient population inversion to achieve lasing. The evidence for such a diversion is the appearance of a long-lived phosphorescence characteristic of the chelate species. None of this type of phosphorescence has been observed from any tetrakis species in the chelates thus far studied.

The absorption constant for the allowed singlet-singlet absorption (the pump band) is exceedingly high, of the order of  $10^5$  to  $10^6\text{ cm}^{-1}/\text{mole} \cdot \text{liter}^{-1}$  and is a severe limitation on the laser performance. An analysis of the pumping situation shows that because of this high value, the effective pump band is narrowed from  $800\text{ \AA}$  to about  $200\text{ \AA}$ .

The correctness of these considerations is shown by a calculation of the threshold. The threshold energy for  $\text{EuB}_4\text{P}$  should be about the same order as that of ruby in the same apparatus and this has been confirmed experimentally.

### 3. PROPERTIES OF THE MATERIAL

#### 3. 1 Solution Chemistry of the Chelates

The lanthanide ions are trivalent and readily form neutral species with three univalent ligands. Such tris chelates are similar to those formed by other hexacoordinating ions such as some transition metals. Because of this similarity, the more complex chemistry of the rare earth ions has often been overlooked. The lanthanides have larger ionic radii and, unlike the transition metal elements, have more vacant orbitals (5d, 6s, 6p) available for bonding. It has recently been shown<sup>3, 10-15</sup> that coordinations larger than 6 can very readily occur.

This work has been limited to the  $\beta$ -diketone chelates of europium. These metal chelates are prepared by using the bidentate ligands in their enolate form. In the resulting compounds the metal ion is bonded to six or eight of the carbonyl oxygens and may coordinate with solvent molecules as well.

A large number of  $\beta$ -diketones have been used as chelating agents, and some of these are listed in Table 1. However, because many of the spectroscopic and chemical characteristics of these are similar, the discussion in this report will be limited to three particular chelates: the benzoyl-acetonate (B), the dibenzoylmethide (D) and the benzoyltrifluoroacetate (BTF).

These chelates can be easily prepared and isolated in the following solid forms:  $\text{EuKe}_3$ ,  $\text{EuKe}_3 \cdot 2\text{H}_2\text{O}$  and  $\text{EuKe}_4\text{P}$ , where Ke represents the bidentate chelating agent and P represents the piperidinium ion (the latter can, of course, be replaced by a number of other unipositive ions). The preparation of these various forms is described in detail in reference 3. The chemical analysis for europium in these chelates is listed in Table II.

TABLE I  
Chelates

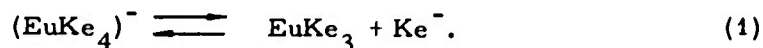
Compound	Formula	Symbol	Reference
Acetylacetone	$\text{CH}_3-\overset{\text{O}}{\parallel}{\text{C}}-\text{CH}_2-\overset{\text{O}}{\parallel}{\text{C}}-\text{CH}_3$	A	9, 16
Benzoylacetone	$\text{C}_6\text{H}_5-\overset{\text{O}}{\parallel}{\text{C}}-\text{CH}_2-\overset{\text{O}}{\parallel}{\text{C}}-\text{CH}_3$	B	1, 3, 9, 13, 17, 18
Trifluoroacetylacetone	$\text{CF}_3-\overset{\text{O}}{\parallel}{\text{C}}-\text{CH}_2-\overset{\text{O}}{\parallel}{\text{C}}-\text{CH}_3$	TFA	19
Benzoyltrifluoroacetone	$\text{CF}_3-\overset{\text{O}}{\parallel}{\text{C}}-\text{CH}_2-\overset{\text{O}}{\parallel}{\text{C}}-\text{C}_6\text{H}_5$	BTF	3, 20
Hexafluoroacetylacetone	$\text{CF}_3-\overset{\text{O}}{\parallel}{\text{C}}-\text{CH}_2-\overset{\text{O}}{\parallel}{\text{C}}-\text{CF}_3$	HFA	11, 14, 19
Dibenzoylmethane	$\text{C}_6\text{H}_5-\overset{\text{O}}{\parallel}{\text{C}}-\text{CH}_2-\overset{\text{O}}{\parallel}{\text{C}}-\text{C}_6\text{H}_5$	D	9, 10, 18, 21
Dibenzoylamine	$\text{C}_6\text{H}_5-\overset{\text{O}}{\parallel}{\text{C}}-\text{NH}-\overset{\text{O}}{\parallel}{\text{C}}-\text{C}_6\text{H}_5$	DA	22
Thenoyltrifluoroacetone	$\text{C}_4\text{H}_3\text{S}-\overset{\text{O}}{\parallel}{\text{C}}-\text{CH}_2-\overset{\text{O}}{\parallel}{\text{C}}-\text{CF}_3$	TTF	23, 24
Thenoylacetone	$\text{C}_4\text{H}_3\text{S}-\overset{\text{O}}{\parallel}{\text{C}}-\text{CH}_2-\overset{\text{O}}{\parallel}{\text{C}}-\text{CH}_3$	T	20
Fuoyltrifluoroacetone	$\text{C}_4\text{H}_3\text{O}-\overset{\text{O}}{\parallel}{\text{C}}-\text{CH}_2-\overset{\text{O}}{\parallel}{\text{C}}-\text{CF}_3$	FTF	20
Fuoylacetone	$\text{C}_4\text{H}_3\text{O}-\overset{\text{O}}{\parallel}{\text{C}}-\text{CH}_2-\overset{\text{O}}{\parallel}{\text{C}}-\text{CH}_3$	F	20

TABLE II  
Chemical Analyses of Chelates

Compound	Percent Metal	
	Theoretical	Experimental
$\text{EuB}_4\text{P}$	17.22	17.35
$\text{Eu}(\text{BTF})_4\text{P}$	13.83	13.70
$\text{EuD}_4\text{P}$	13.44	13.26
$\text{Eu}(\text{BTF})_3 \cdot 2\text{H}_2\text{O}$	18.24	18.20
$\text{EuD}_3 \cdot \text{H}_2\text{O}$	17.72	17.54
$\text{EuB}_3 \cdot \text{H}_2\text{O}$	23.26	23.47
$\text{EuB}_3$ (anh.)	23.92	24.10
$\text{EuD}_3$ (anh.)	18.50	18.49

Solutions of these chelates give rise to a variety of molecular species depending on the solvent. We have confined our studies to four solvents. The first is a mixture of ethanol and methanol in the ratio of 3:1, the second is the former mixture with dimethylformamide in the ratio of 4:1, the third is a 9:1 mixture of dimethylformamide and methanol, and the fourth is acetonitrile. These are good solvents for the chelates, and the first two have the property of glassing as the temperature is decreased, so they can be used for spectroscopic studies and laser experiments at low temperatures. In these solvents, the anhydrous and hydrated tris chelates produce essentially the same species. In the alcohol solvent six orbitals are used for bonding to the ligand oxygens and either two or all three of the remaining ones to the alcohol oxygens. In the dimethylformamide solvent it is the oxygens of this compound that use the remaining orbitals.<sup>3</sup> The latter two solvents are used for experiments in the region of room temperature, and although the same kind of interactions occur, much less is known about the details of the solvent coordination.

The tetrakis form of the chelate dissociates according to the equation



This dissociation occurs to varying degrees in the first two solvents as shown in Table III.<sup>8</sup> In both cases, the tris forms are solvated as described above; in addition, in the dimethylformamide solvent, the tetrakis form also solvates, accepting a pair of electrons from the dimethylformamide oxygen to form a nine-coordinated compound. The tendency for this to occur depends on the strength of the Lewis base that is providing the electrons and on the type of chelating agent. Much of the information on the chemistry of these solutions has been obtained from spectroscopic studies, particularly the fluorescence emission spectra of the europium ion. This will be described in more detail in the next section.

TABLE III  
Degree of Dissociation

Chelating Agent	Solvent	
	Alcohol	DMF
B	0.37	0.82
D	0.43	0.51
BTF	1.00	0.47

### 3.2 Spectroscopic Properties of the Chelates

The spectroscopy of the chelates is characterized by both their organic and inorganic components. The two principal features are the intense absorption typical of the organic part and the intense fluorescence emission of the europium ion. The significance of absorption has already been mentioned and is discussed at length in references 1 and 2. In this section only the ion fluorescence will be discussed,\* primarily the emission to the  ${}^7\text{F}_0$ ,  ${}^7\text{F}_1$  and  ${}^7\text{F}_2$  levels. The most intense emission (about

\* The problem of fluorescent decay time has been discussed at length in the Technical Summary Report of 1963 and in references 1 and 25.

95 percent of that occurring to these levels) is observed in the  ${}^5D_0 - {}^7F_2$  transition and occurs between 6100 Å and 6250 Å. The  ${}^5D_0 - {}^7F_1$  emission is found between 5850 Å and 6000 Å and the  ${}^5D_0 - {}^7F_0$  emission between 5790 and 5810 Å.

The details of the emission in each of these regions have been used to provide information on the symmetry of the species involved, the number of species present, and the extent of dissociation in the tetrakis form of the chelate. This will be illustrated in some detail for the  $\text{EuD}_4\text{P}$  chelate. Figure 1 (a) shows the spectrum of the four-fold form. It is seen that there are three lines and a long wavelength tail in the  ${}^5D_0 - {}^7F_2$  region, six easily identifiable lines in the  ${}^5D_0 - {}^7F_1$  region, and two in the  ${}^5D_0 - {}^7F_0$  region. For the latter two transitions, there are more lines than would be allowed for a single species even if the degeneracies were completely removed. The spectrum of the tris chelate, shown in Fig. 1 (b), is even more complex, with eight lines in the long-wavelength region, six in the center one, and two in the  ${}^5D_0 - {}^7F_0$  region. The latter spectrum can only be interpreted if it is assumed that there are at least two species present. These species can arise from different degrees of solvation or from different orientations of the solvating molecules; in either case, the excess number of lines can be readily accounted for.

The key to the tetrakis spectrum is found in the  ${}^5D_0 - {}^7F_0$  transition. One of the two lines falls exactly where the strong line of the tris spectrum is found, while the other line appears only in the tetrakis spectrum. If it is assumed that this coincidence means that there is tris chelate present in the solution of the tetrakis chelate, the amounts can be estimated from the relative intensities of the lines in the two spectra. This depends on the fact that the absorption band of the chelate is, to a very good approximation, simply the absorption band of the enolate ion of the chelating agent itself multiplied by the number of ligands per chelate molecule.<sup>18</sup> If  $f$  represents the fractional dissociation (according to Eq. (1) ) and

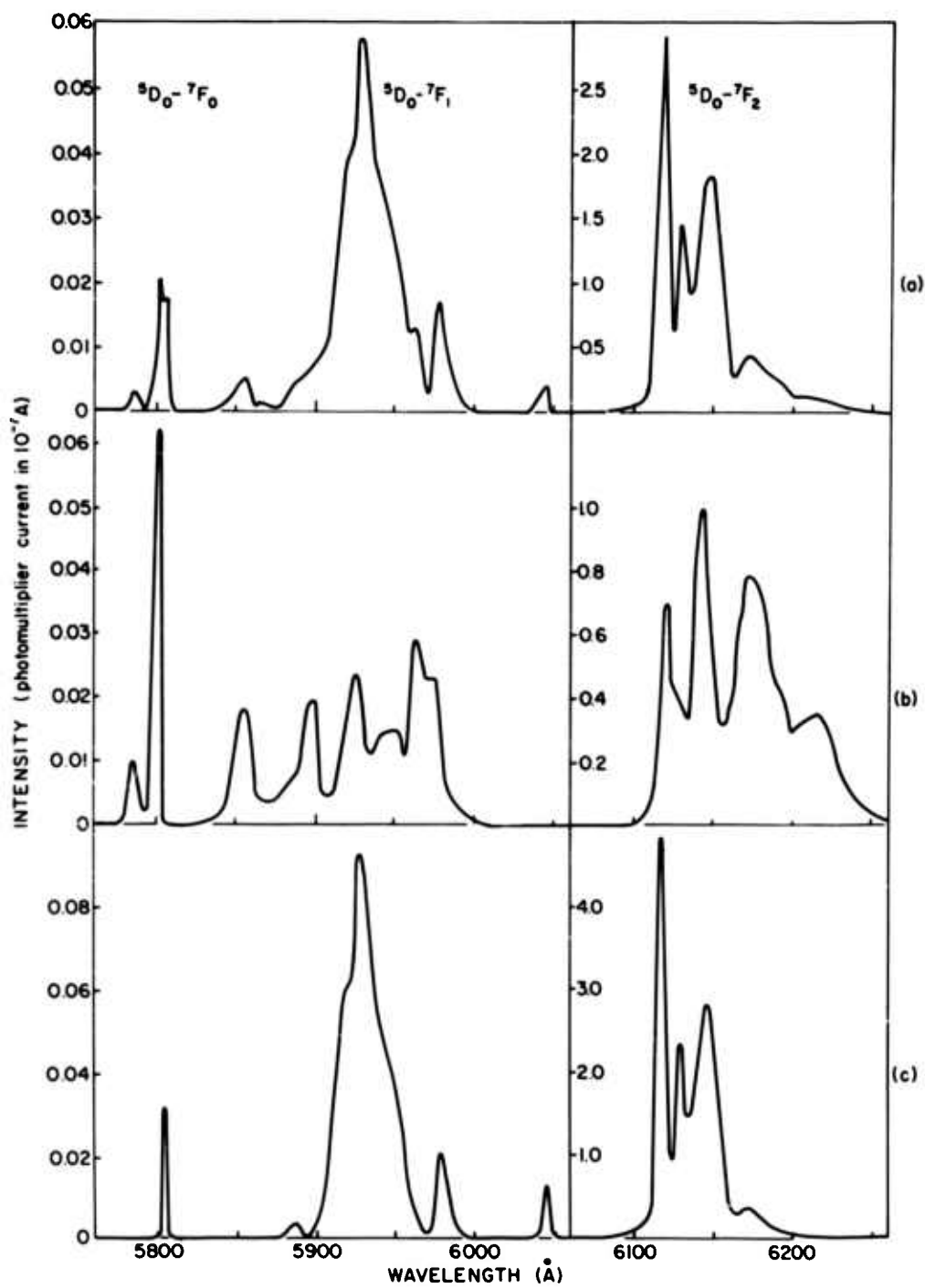


Fig. 1. Emission spectra of europium dibenzoylmethide in alcohol solution: (a) Tetrakis form, uncorrected; (b) Tris form; (c) Tetrakis form, corrected for dissociation.

$\alpha$  the absorption constant per mole of ligand, then the probability of exciting the tris chelate molecule in a solution containing all the species in Eq. (1) is given by

$$P = \frac{\frac{3f}{4}}{\frac{3f\alpha}{4} + \frac{f\alpha}{4} + (1-f)\alpha} = \frac{3f}{4} \quad (2)$$

In solutions containing only three ligand species, this probability is unity.

Assuming that all the photons entering the liquid sample in the region of the extremely intense absorption band are totally absorbed, then the intensity of emission from the three-ligand species is directly proportional to the probability  $p$ . If we, therefore, let  $r$  represent the ratio of the intensity of the three ligand emission from the solution of the partially dissociated four ligand material to the intensity from an equivalent solution of pure tris material, we find that

$$r = \frac{3}{4} f. \quad (3)$$

Equation (3) enables us to determine the degree of dissociation and to correct the emission from the nominal tetrakis form to get the true tetrakis spectrum. This is shown in Fig. 1 (c). It is seen that this correction virtually eliminates the tail in the long-wavelength region and simplifies the spectrum in the  ${}^5D_0 - {}^7F_1$  region. The appearance of two sharp lines and one broad one is consistent with the selection rules for a site symmetry of  $S_4$  for the europium ion. This is the symmetry that is obtained from a slight distortion of the  $D_{2d}$  dodecahedral arrangement of the eight oxygens. The equivalent set of spectra are shown for  $\text{EuB}_4\text{P}$  in Fig. 2. In this case, since there is only one sharp line and one broad one, the site symmetry of the europium ion is consistent with  $D_{2d}$ . The symmetry groups and the selection rules for the  ${}^5D_0 - {}^7F_2$  transition in the various types of eight-fold coordination are given in Table IV and discussed in more detail in reference 26. In the case of BTF two different compounds, one of which analyzes to  $\text{Eu}(\text{BTF})_4\text{P}$  and the other to  $\text{Eu}(\text{BTF})_3$ , give identical spectra, as is seen in Fig. 3. The spectrum due to the former is only 3/4 as intense

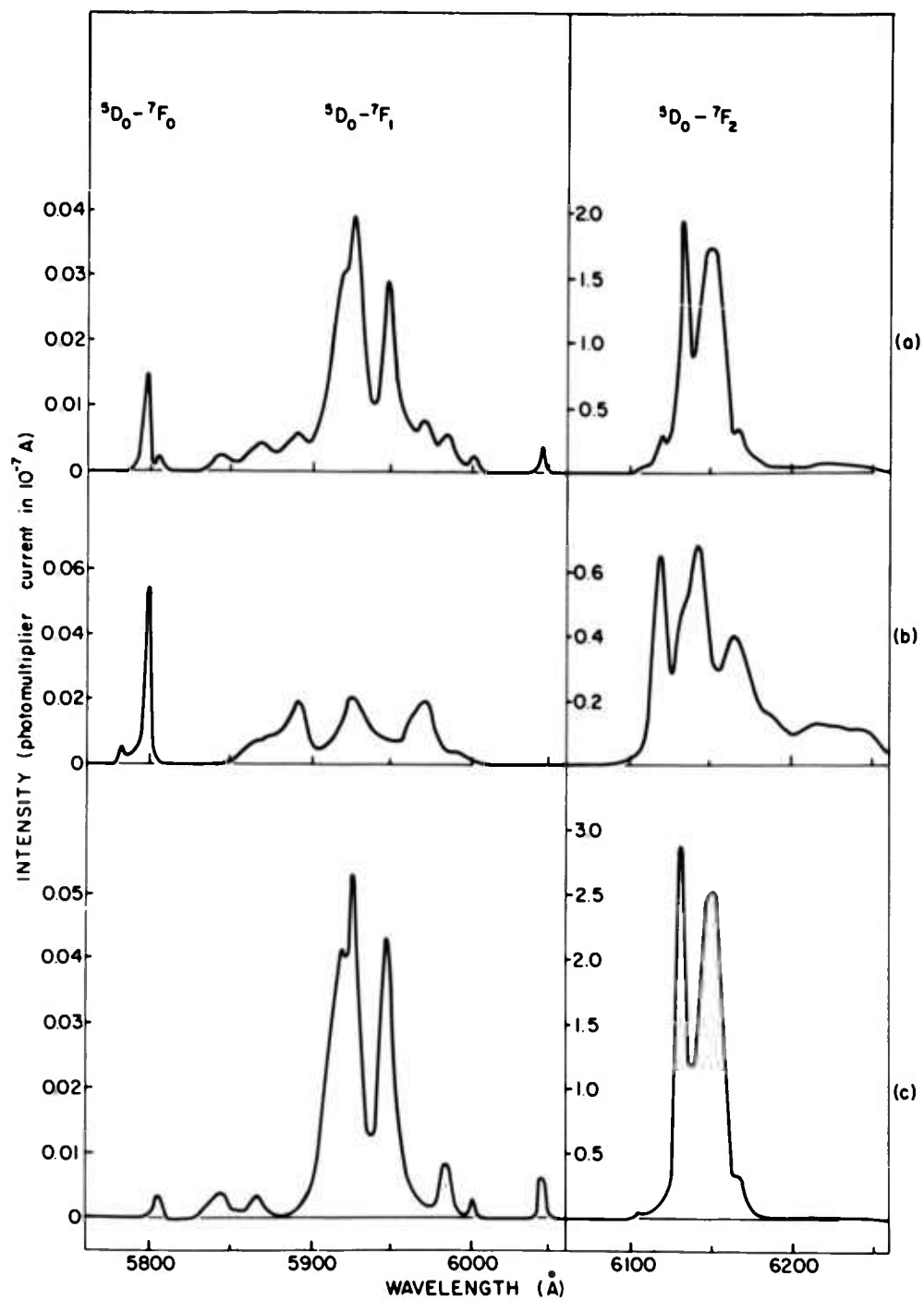


Fig. 2. Emission spectra of europium benzoylacetonate in alcohol solution: (a) Tetrakis form, uncorrected; (b) Tris form; (c) Tetrakis form, corrected for dissociation.

TABLE IV.

Electric Dipole Selection Rules Of Europium  
Transitions For Various Coordination Structures

Spatial Configuration	Site Symmetry	Active Representations		
		${}^5D_0 - {}^7F_2$	${}^5D_0 - {}^7F_1$	${}^5D_0 - {}^7F_0$
Face-centered Isosceles prism	<u><math>C_{2v}</math></u>	$A_1, A_1, B_1, B_2$	$A_1, B_1, B_2$	$A_1$
	$C_2$	$A, A, A, B, B$	$A, B, B$	$A$
Archimedean Antiprism	<u><math>D_{4d}</math></u>	none	$B_2, E_1$	none
	$D_4$	$E$	$A_2, E$	none
	$D_2$	$B_1, B_2, B_3$	$B_1, B_2, B_3$	none
Tetragonal Dodecahedron	<u><math>D_{2d}</math></u>	$B_2, E$	$B_2, E$	none
	$S_4$	$B, B, E$	$B, E$	none
	$D_2$	$B_1, B_2, B_3$	$B_1, B_2, B_3$	none
Nine-fold Antiprism Adduct	<u><math>C_{4v}</math></u>	$A_1, E$	$A_1, E$	$A_1$
	$C_4$	$A, E$	$A, E$	$A$
	$C_2$	$A, A, A, B, B$	$A, B, B$	$A$

Symmetries that are underlined are the highest ones for the oxygens alone; the others are subgroups derived from them by placement of the ligand bridges or steric distortion.

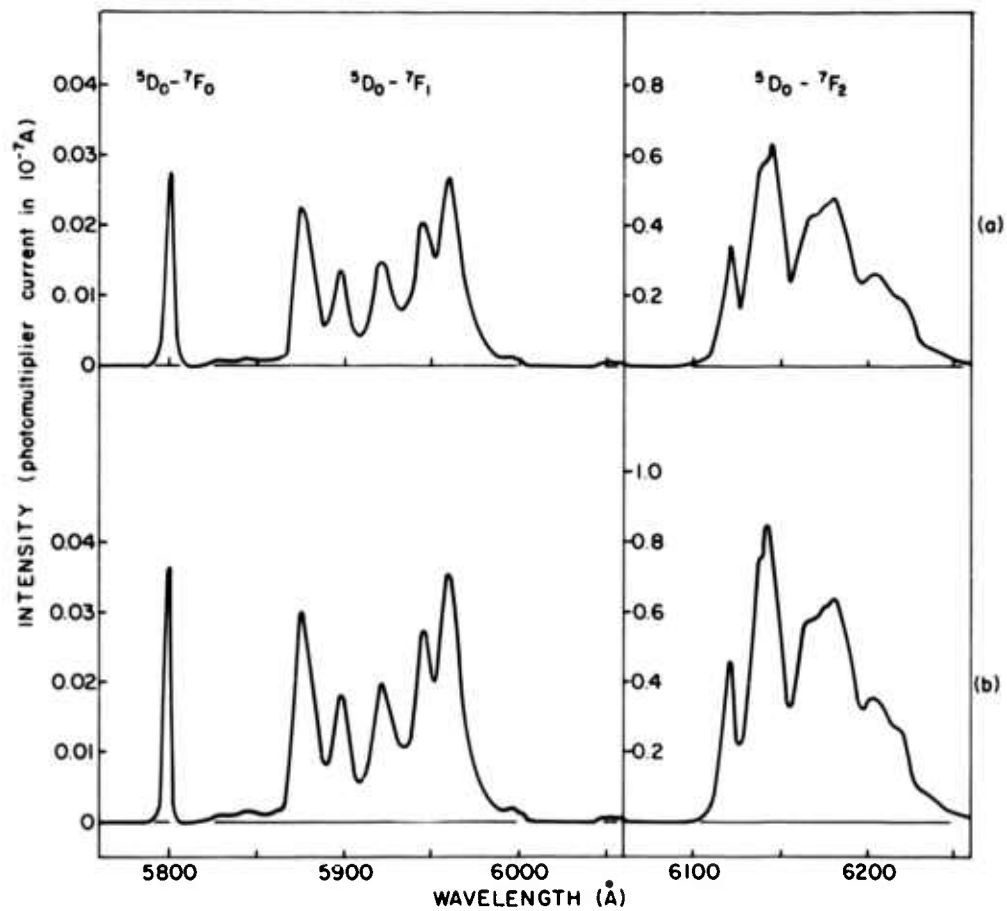


Fig. 3. Emission spectra of europium benzoyltrifluoroacetate in alcohol solution: (a) Tetrakis form, uncorrected; (b) Tris form.

as that of the latter and this is consistent with the idea that the tetrakis chelate is completely dissociated in the alcohol solvent. The degrees of dissociation for these chelates in alcohol solution are given in the first column of Table III.

### 3.3 Solvent and Salt Effects

Since the solvent can affect the equilibrium existing in solution and the types of molecular species present, it is reasonable to expect pronounced solvent effects in the spectroscopic properties of the chelate solutions. Thus, when dimethylformamide is added to the alcohol solvent, the spectroscopic picture is altered. The tetrakis form of  $\text{EuD}_4\text{P}$  again dissociates, and the corrected spectra are shown in Fig. 4. In this case there are only two lines, one sharp and one broad. This is consistent with the selection rules derived for a site symmetry  $C_{4v}$ . This is the symmetry that would be expected if the dimethylformamide oxygen added axially and displaced the other eight so that they formed an Archimedean antiprism. The same sort of effect is seen in Fig. 5 for  $\text{EuB}_4\text{P}$ . In the case of the BTF chelate, the spectra of which are shown in Fig. 6, the equilibrium of Eq. (1) has been displaced to the left so that the dissociation is no longer complete. The degrees of dissociation in this solvent are given in the second column of Table III.

If the solvent for  $\text{Eu}(\text{BTF})_4\text{P}$  is now changed to acetonitrile and the temperature range elevated to between 250 and 300°K, the spectra obtained is illustrated in Fig. 7. In this case it is noteworthy that the tetrakis form of the chelate is less than 10 percent dissociated, as can be seen from the  $^5\text{D}_0 - ^7\text{F}_0$  portion of the spectra, and that the peak intensity of the four-fold form is comparable to that of many chelates at lower temperatures, even though the emission has a greater line width. The precise nature of the interaction with acetonitrile is not fully understood, but may be related to coordination with the nitrogen of the nitrile group.

A further important and interesting type of interaction is that due to different cations. In all the work described to this point, the cation associated with the tetrakis chelate anion was piperidinium. If this is changed

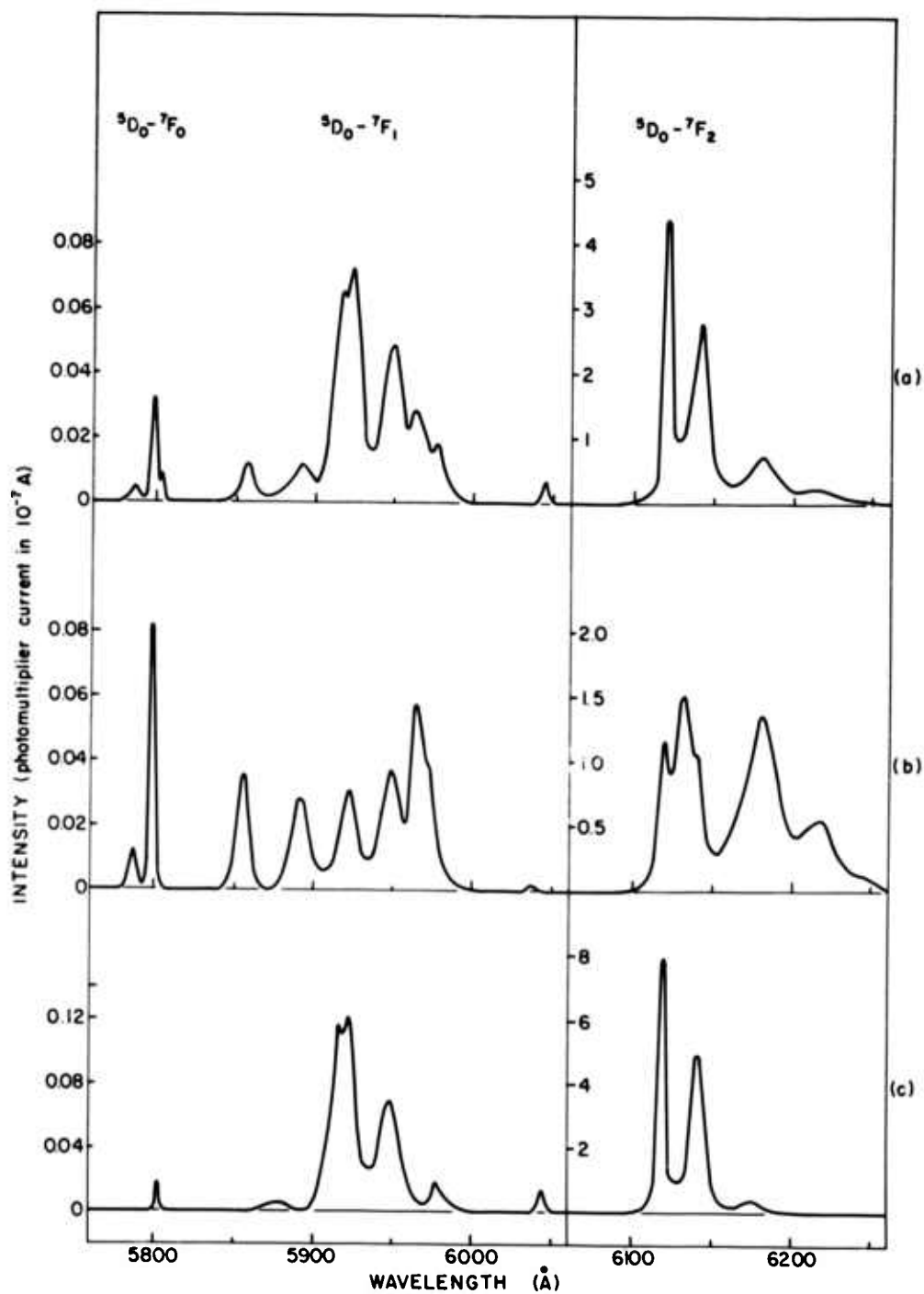


Fig. 4. Emission spectra of europium dibenzoylmethide in DMFA solution: (a) Tetrakis form, uncorrected; (b) Tris form; (c) Tetrakis form, corrected for dissociation.

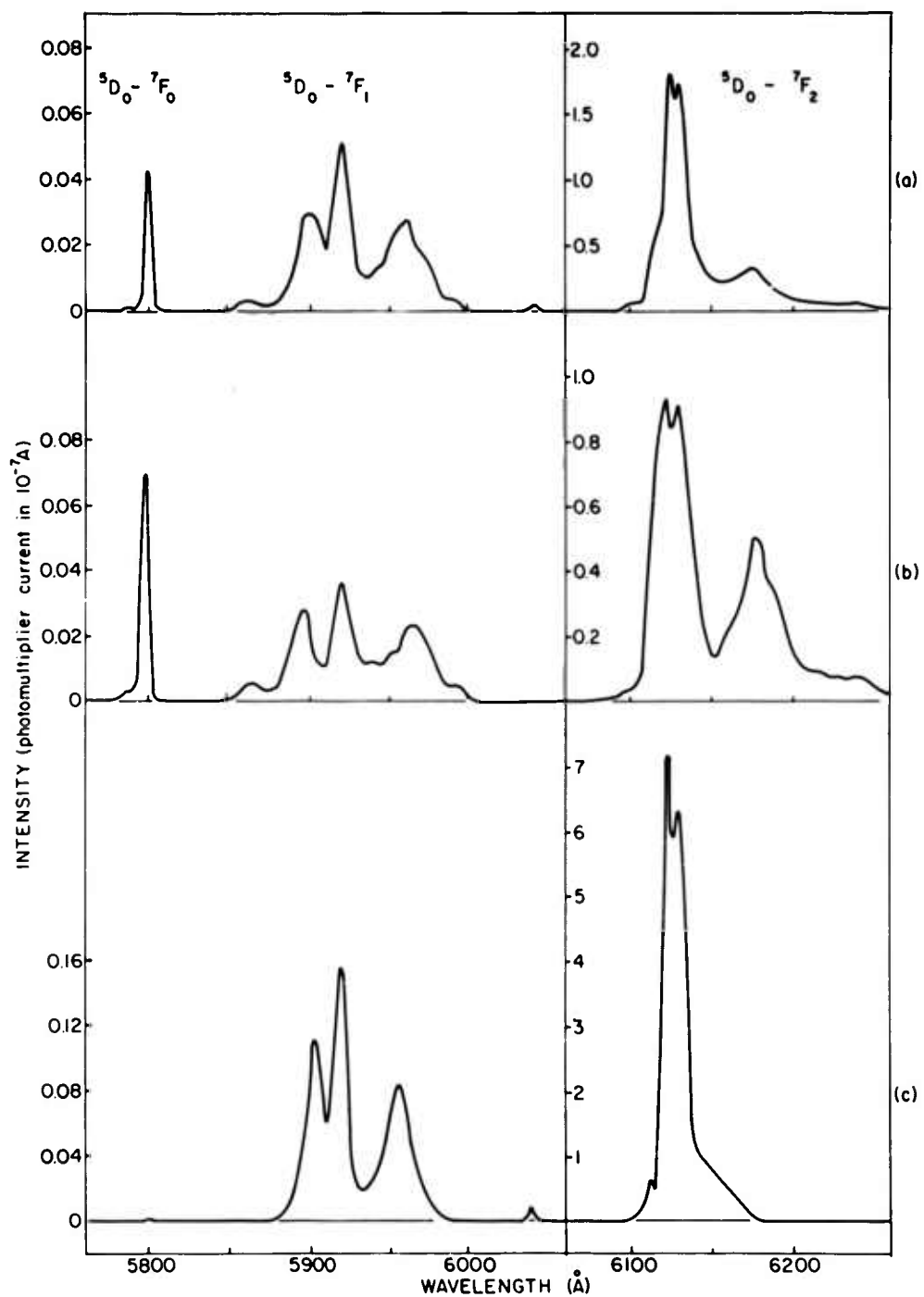


Fig. 5. Emission spectra of europium benzoylacetonate in DMFA solution: (a) Tetrakis form, uncorrected; (b) Tris form; (c) Tetrakis form, corrected for dissociation.

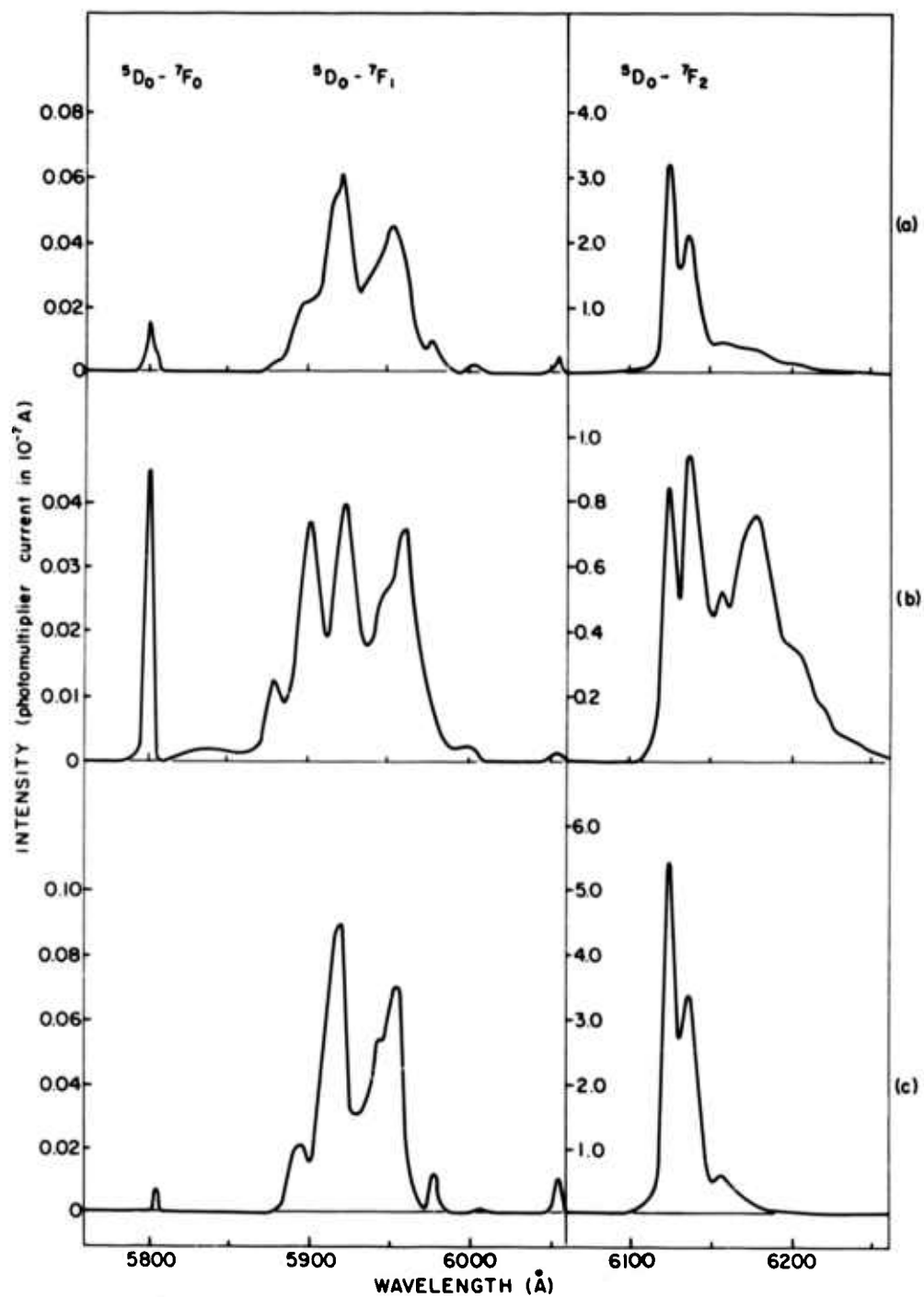


Fig. 6. Emission spectra of europium benzoyltrifluoroacetate in DMFA solution: (a) Tetrakis form, uncorrected; (b) Tris form; (c) Tetrakis form, corrected for dissociation.

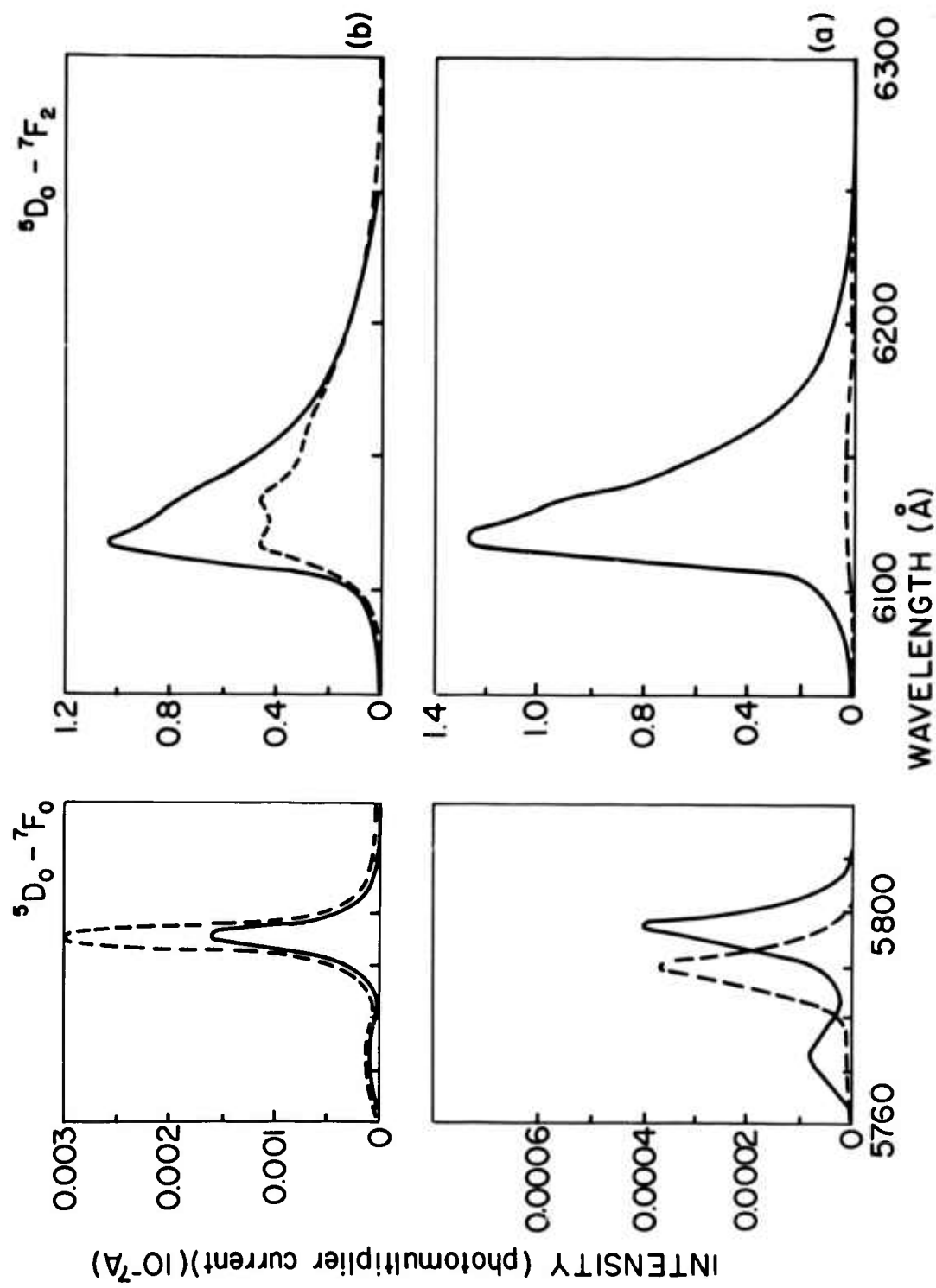


Fig. 7. Fluorescence emission spectrum of an 0.01 M solution of  $\text{Eu}(\text{BTF})_4\text{P}$  in (a) acetonitrile (b) dimethylformamide at  $25^\circ\text{C}$ . In each case the solid line is the tetrakis form and the dotted line the tris form of the chelate.

to an alkali cation, a rather striking effect, first observed by Meyer, Poncet, and Verron,<sup>27</sup> can be observed. The principal emission decreases, and a new emission frequency appears at 6114 Å. Increasing the molar ratio of cation to chelate anion produces a uniform change continuing in the direction of increasing 6114 Å intensity, as indicated in Fig. 8. This effect occurs with all alkali-type cations including  $\text{NH}_4^+$ , but is most pronounced with the sodium ion.

As in the case of acetonitrile, the precise nature of the interaction of the singly positive cation with the chelate is not clear. In this case, the appearance of a single intense emission peak suggests that the symmetry of the anion approaches  $D_4$  (see Table IV) which would require the addition of a sodium ion at opposite ends of the  $C_4$  axis of an Archimedian antiprism. This in turn suggests a ten-fold coordinated europium ion, although this coordination need not be covalent.

The effect of the cation additive is not limited to low temperatures, but can be seen even at room temperature. In a solvent consisting of a 9:1 ratio of dimethylformamide to methanol and a 4:1 ratio of cation to chelate anion, the spectrum illustrated in Fig. 9 is obtained. This is to be compared with that obtained without the addition of  $\text{Na}^+$  also illustrated in the same figure. Again, a similar effect is seen: the intensification of the spectrum and the intensification of one of the  $^5D_0 - ^7F_2$  transitions relative to the others.

### 3.4 Effects on Laser Action

All the changes in the spectroscopic behavior of these solutions have pronounced effects on the laser behavior of the solutions. In this section, such laser effects will be correlated with the spectroscopy, and a pattern will emerge that indicates, at least for the europium chelates, the most advantageous environments.

From the spectra in Figs. 1 - 6 it is readily seen that the tetrakis form has a higher peak intensity than the tris form in both the alcohol and dimethylformamide solvents. The spectra of both forms are more intense in dimethylformamide, but the increase in intensity of the tetrakis form is greater. The relative intensities of the peaks of the B and D chelates are given in Table V.

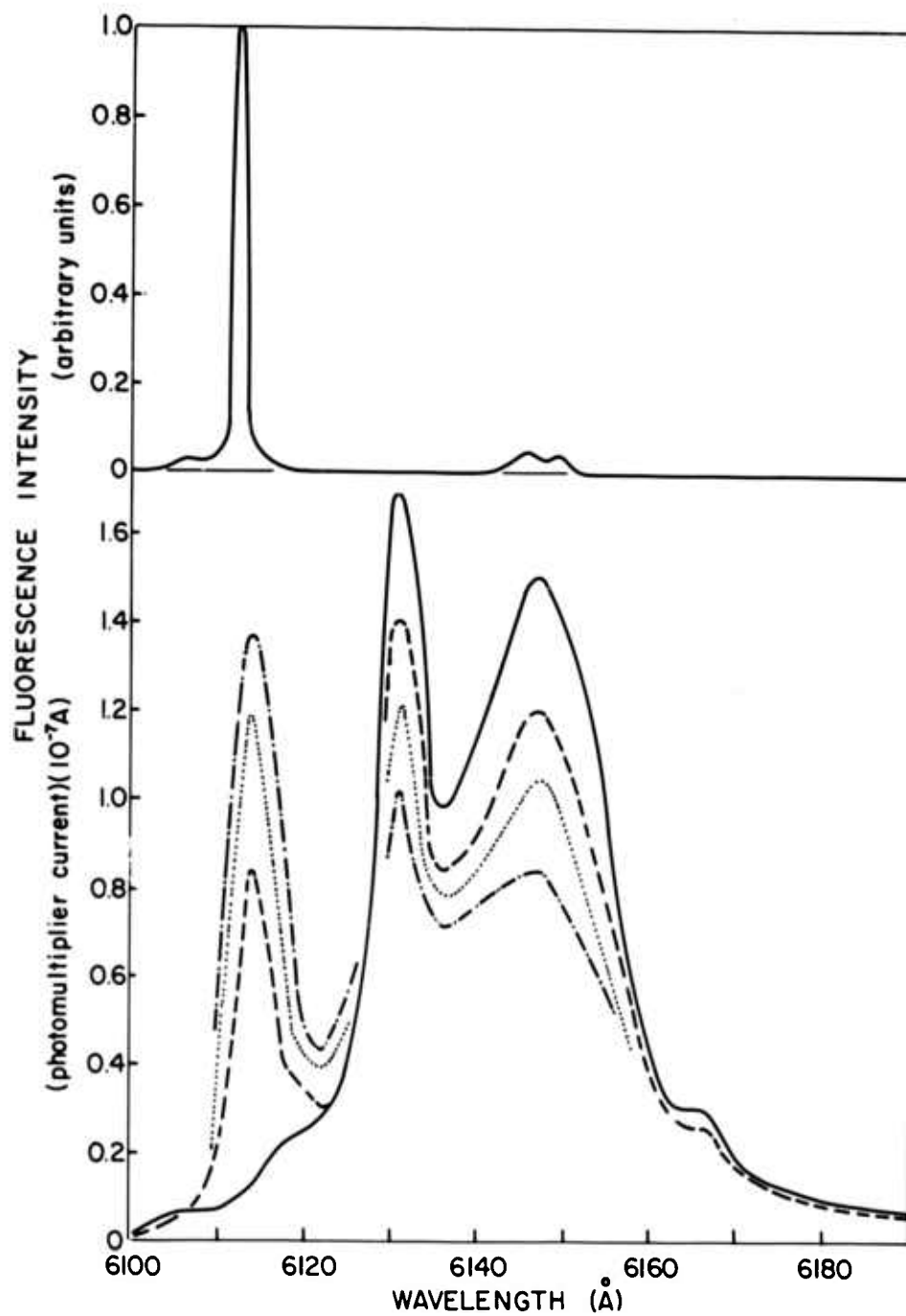


Fig. 8. (a) Fluorescence emission spectra of 0.01M  $\text{EuB}_4\text{P}$  in alcohol at  $-150^\circ\text{C}$  with various concentrations of sodium acetate: — none; --- 0.005M; .... 0.01M; -·-·- 0.015M. (b) Fluorescence emission spectrum of solid adduct at  $-150^\circ\text{C}$ .

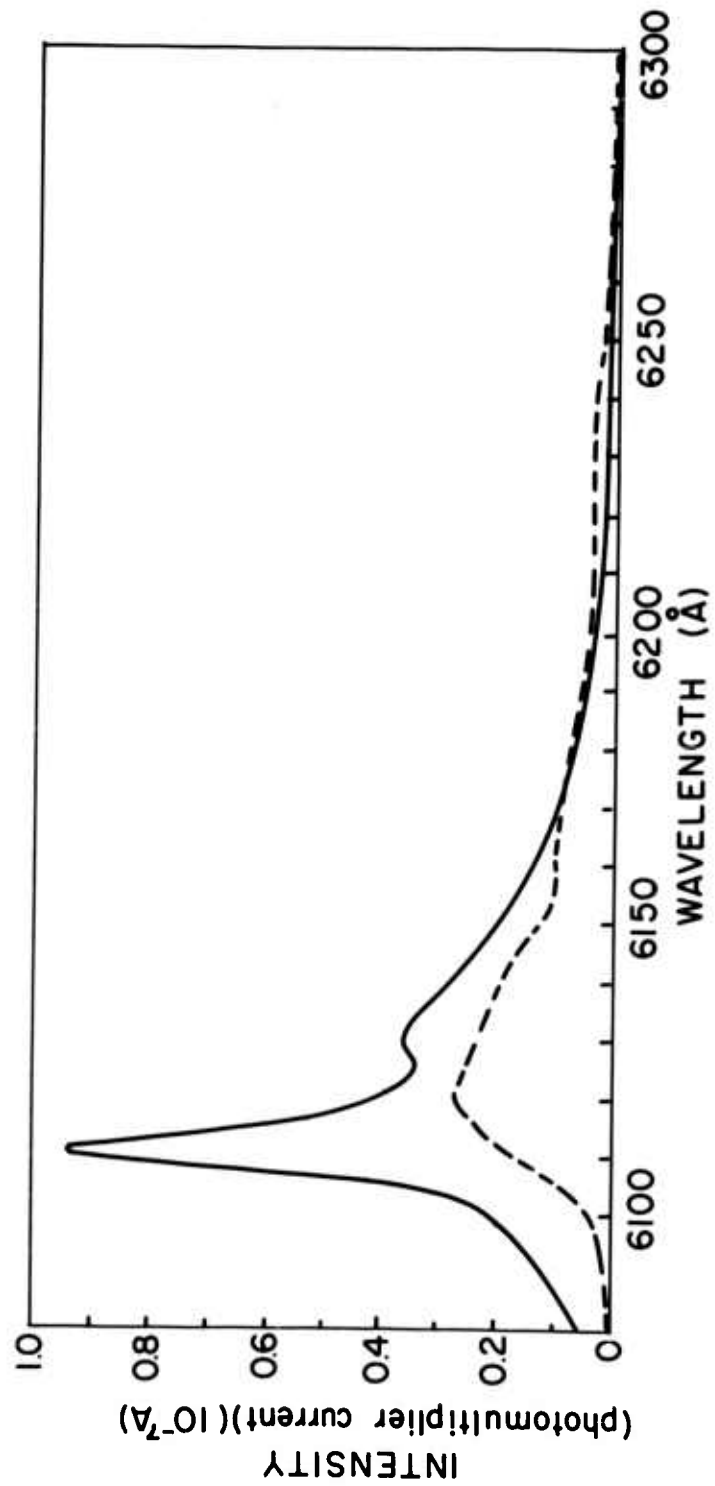


Fig. 9. Fluorescence emission spectra of  $\text{EuB}_4\text{P}$  in dimethylformamide-methanol solvent in the ratio 9:1. Temperature,  $-40^\circ\text{C}$ ; concentration 0.01M; — with 0.04M Na acetate added, ---- with no Na acetate.

TABLE V  
Comparison of Peak Intensities

Chelating Agent	Solvent			
	Alcohol		DMF	
	Tris	Tetrakis	Tris	Tetrakis
B	0.7	2.75	0.9	6.30
D	1.0	3.20	1.5	7.90
BTF	-	-	0.95	5.40

From a laser point of view, it is evident that the tetrakis forms are more desirable than the tris forms, and that from a consideration of the spectrum of the tetrakis form alone, dimethylformamide is the better solvent. However, this advantage may be offset by the increased degree of dissociation. For example, laser action is readily observed with  $\text{EuB}_4\text{P}$  in both solvents, but in dimethylformamide, despite the apparently more favorable spectrum, the threshold is much higher. This is a consequence of the increased degree of dissociation which is detrimental in two ways. It not only decreases the concentration of active species, but also decreases the effective pumping, since the products of the dissociation absorb pump energy as effectively as the active species and contribute nothing to the useful fluorescence.

In the case of  $\text{EuD}_4\text{P}$  the reverse effect is seen. In the alcohol solvent some evidence of laser action has been occasionally observed at very high thresholds, but these results lack reproducibility. In the dimethylformamide solvent, on the other hand, laser action is readily obtained at thresholds not much higher than with  $\text{EuB}_4\text{P}$  in an alcohol solvent. The appearance of laser action in  $\text{EuD}_4\text{P}$  in the dimethylformamide solvent is due to the better spectroscopic properties of the nine-fold-coordinated compound and the fact that in this case the degree of dissociation increases only slightly. As a result, the advantage gained in the emission spectrum is not overcome by the dissociation.

The chelate  $\text{Eu}(\text{BTF})_4\text{P}$  presents a more striking illustration of the efficacy of the tetrakis form of the compound. In ethanol, where the compound is 100 percent dissociated, no laser action can be obtained. However, in the dimethylformamide solvent when there is an appreciable fraction of the four-fold chelate (~52 percent) laser action at reasonable thresholds can be observed in solutions where temperature is as high as  $210^\circ\text{K}$ . At these temperatures (about that of dry ice), the solvent is quite fluid. At more elevated temperatures, the degree of dissociation increases further, and no laser action can be obtained either in a mixture of alcohol and dimethylformamide or pure dimethylformamide.

A different behavior is observed in acetonitrile. In this solvent the BTF chelate is in the tetrakis form to the extent of 90 percent even at temperatures as high as  $300^\circ\text{K}$ . Because of the great fluorescence intensity characteristic of these highly coordinated compounds, particularly those containing fluorine, laser action is observed at room temperature and can perhaps be observed at even higher temperatures.<sup>28</sup> This then represents the achievement of laser action in a fluid medium without any cooling.

These results can be summarized in the following manner. While the details of the spectroscopic behavior of the europium  $\beta$ -diketone chelates varies as the structure of the ligand is altered, many features remain similar. Thus, the  $^5\text{D}_0 - ^7\text{F}_2$  transition is always the most intense, and, for a given chelating agent, the tetrakis form always has a more intense emission than the tris form.

There are, however, other factors that are not so consistent. The degree of dissociation of the tetrakis chelate is roughly correlated with the acid strength of the ligand in the keto form, but quantitative predictions cannot be made. The effect of altering the solvent appears to be even less predictable, and there is too little information for establishing any empirical rule. These factors have to be determined for each individual case and the examples cited above serve to illustrate the effects that can be expected.

The salt effects apparently represent another class of phenomena. From the spectroscopy, these appear to be a result of a more drastic alteration of the structure. In the alcohol solvent, at low temperatures, the appearance of the single sharp line is indicative of a new species. At intermediate salt concentrations, when both species are present, laser action can be achieved in either of the two dominant lines, as seen in Fig. 10. At higher sodium concentrations, laser action is seen only in the new line. This is a first example of the "tuning" of the laser emission frequency by a simple structural change.

If the solvent is changed the salt effect can be pursued to higher temperatures. In a 9:1 dimethylformamide to methanol solvent a relatively sharp and intense line is observed nearly to room temperature. This line is due primarily to the tetrakis complex, and laser action can be observed up to temperatures between 240°K and 245°K. Above this temperature, dissociation has proceeded to too great an extent.

The effect of these cations appears to be applicable only to the  $\text{EuB}_4\text{P}$  chelate. This may be a steric effect since the substituents on the other ligands studied are bulkier and may keep the alkali ion from penetrating close enough to the europium to exert any influence. The exact nature of the salt effect requires further study.

#### 4. PROPERTIES OF THE LASER

##### 4.1 General Considerations and Experimental Arrangement

At least three conditions must be met to obtain laser action in the chelates. First, a minimum concentration of active species and degree of inversion (determined by spectroscopic parameters and cavity losses) must be attained. Secondly, the rate of pumping must be high enough to achieve and maintain the required inversion. This is essentially a kinetic problem in which one has to take into account the rates of the various processes. Finally, one must consider the process of absorption by which pumping is achieved. This enables us to compute the threshold for laser action. We will discuss all these problems in turn.

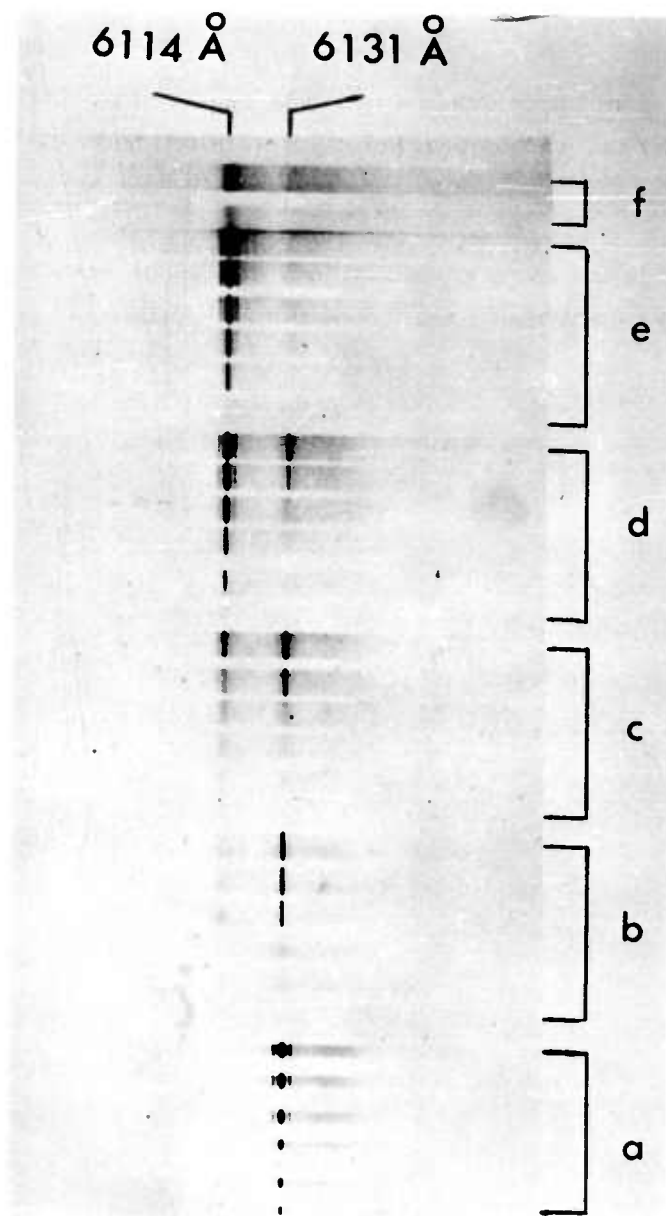


Fig. 10. Emission spectra of 0.01M  $\text{EuB}_4\text{P}$  in alcohol at  $-150^\circ\text{C}$  with various input energies to the flash tube and different concentrations of sodium acetate: (a) none, (b) 0.005M, (c) 0.0075M, (d) 0.010M, (e) 0.0125M, (f) 0.015M.

In (a) - (e) the flash input energies from bottom to top within each group are 2500, 3000, 3500, 4000, 4500, and 5000 joules. In (f), where precipitation prevented stimulated emission, only 4000- and 5000-joule flashes are shown. All spectra were taken with a single input pulse to the flash tube and with 50-micron slits. The weaker lines visible on each side of the laser emission are ghosts due to the grating.

The minimum concentration which is required to obtain oscillation is expressed by the well-known Schawlow-Townes relation<sup>29</sup>

$$\Delta n \geq \frac{p\tau_r}{t_c}; \quad p = \frac{4\pi^2\delta\lambda'}{\lambda'^4}, \quad (4)$$

where  $\Delta n$  is the excess population in the upper state,  $p$  the number of modes under the fluorescent line,  $t_c$  the cavity lifetime,  $\lambda'$  and  $\Delta\lambda'$  the wavelength and halfwidth of the laser line, and  $\tau_r$  the radiative lifetime. All these quantities except  $t_c$  are known from the spectroscopic measurements. In the original experiments  $t_c$  was estimated to be  $\sim 5 \times 10^{-9}$  sec.<sup>10</sup> This result leads to a  $\Delta n \approx 5 \times 10^{18}$  per  $\text{cm}^3$ , which is well within the solubility limit of  $\text{EuB}_4\text{P}$  in alcohol at low temperature. The optical properties of a viscous (low temperature) solution are quite good, but losses induced by the heating caused by the flash could be very large. The distortion of the rays in a cavity due to refractive index gradients have been considered by Winston and Gudmundsen,<sup>30</sup> who concluded that laser action will be very difficult to achieve in liquid systems. The rate of change of refractive index with temperature is of the order of  $-4 \times 10^{-4}$  (degrees)<sup>-1</sup> for alcohol at room temperature,<sup>31</sup> a factor of about 30 larger than for ruby. Although refractive index gradient losses undoubtedly exist, they can be shown to be surprisingly small at least for a time sufficient to build up the field intensity in the cavity.

In considering the kinetics of optical pumping of pulsed lasers, one has to make a decision on the approximation to be used. For continuous lasers, steady-state considerations are obviously applicable. This also holds reasonably well when the duration of the exciting pulse is longer than the lifetime of the fluorescence, although somewhat different considerations apply when the pulse is very much shorter than the lifetime. In most of our experiments the flash was about twice as long as the lifetime, and we shall deal with the kinetics from the steady-state point of view. A more precise calculation would involve a numerical solution of the rate equation, but this does not seem to be justified for the present.

The rate equations are set up in terms of the probabilities defined on the energy level diagram of Fig. 11. The solution has been carried out in Ref. 30 where it is shown that to obtain an inversion  $\Delta n$ , the pumping

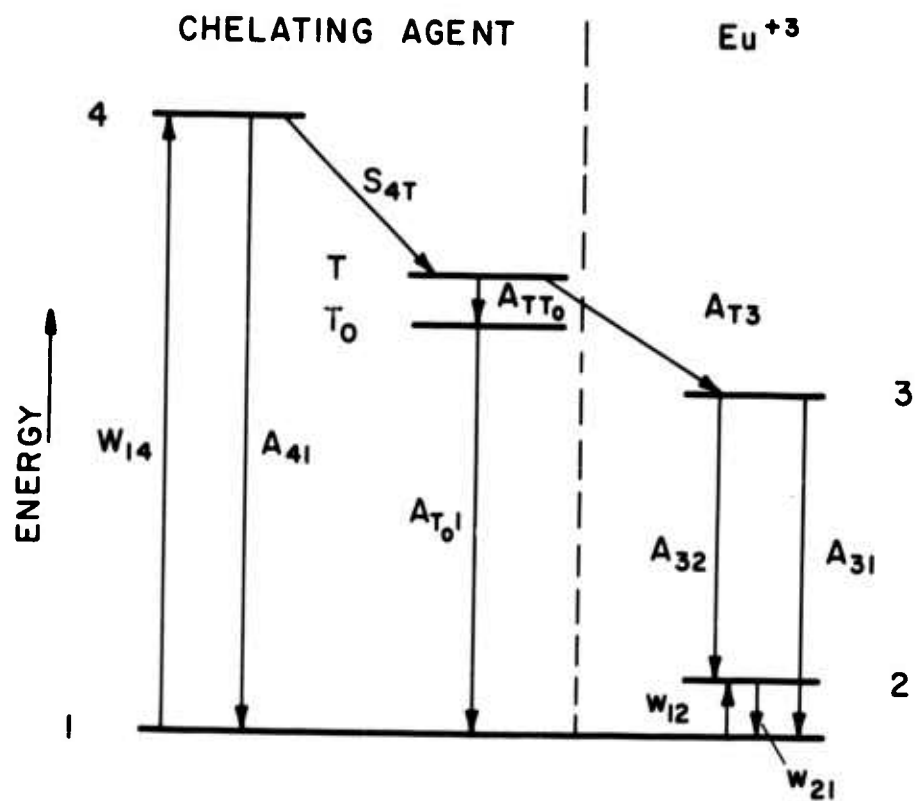


Fig. 11. Energy level diagram of a europium chelate. The levels are:  
 1 - ground state  
 2 - terminal state of laser transition  
 3 - upper state of laser transition  
 T, T<sub>0</sub> - triplet states of the ligand  
 4 - excited singlet state of the ligand  
 A's are transition probabilities between designated levels  
 S<sub>4</sub>T is the intersystem transition probability

probability (proportional to the light intensity falling on the sample) must be

$$W_{14} \geq \frac{A_3 \frac{\Delta n}{N_0}}{\eta(1-b) \frac{\Delta n}{N_0}}, \quad (5)$$

where  $A_3$  is the decay time of level 3 and

$$\frac{1}{\eta} = 1 + \frac{A_{TT_0}}{A_{T3}} \quad (6)$$

$$b = 1 + \frac{A_3}{A_{T_01}} \frac{A_{TT_0}}{A_{T3}}.$$

It is evident from Eq. (5) that even when the pumping rate is infinite there is a maximum value of  $\Delta n$

$$(\Delta n)_{\max} = \frac{N_0}{1 + \frac{A_{TT_0}}{A_{T3}} \frac{A_3}{A_{T_01}}}. \quad (7)$$

We now have to consider the possible values of the terms in the denominator. The phosphorescence decay is usually appreciably longer than that of the ion level, and therefore  $A_3/A_{T_01} \gg 1$ . Unless the branching ratio  $A_{TT_0}/A_{T3}$  is extremely small, the maximum value of  $\Delta n$  will be much too small. For example, if  $A_{TT_0}/A_{T3}$  is of the order of 0.1 (90 percent transfer efficiency from triplet T to the ion), and if  $A_3/A_{T_01} \approx 100$ , then  $(\Delta n)_{\max}$  may be less than ten percent of  $N_0$ . In such a case the solubility of the cheiate at low temperature may be insufficient to obtain the minimum required concentration. It is therefore particularly important to pay attention to the existence of organic phosphorescence. This indicates the possibility of a non-zero branching ratio, which can seriously affect the possibility of obtaining the necessary inversion. Even if the phosphorescence is absent, we cannot necessarily conclude that the energy transfer from the triplet to the ion is one hundred percent efficient. In such cases

the branching ratio may still be finite ( $A_{T_0}/A_{T_3} > 0$ ) but there may exist a rapid nonradiative deactivation of the lowest triplet state. The parameter  $1/\eta$  would be a measure of the efficiency of energy transfer.

The rate of pumping is obtained by multiplying the probability  $W_{14}$  by the population of the ground state

$$R = W_{14} N_0 = \frac{A_3 \Delta n}{\eta} \quad (8)$$

This rate is directly related to the flux  $F^0(\lambda)$  measured in watts/cm<sup>2</sup> per unit wavelength interval. The flux must be incident on the surface of the sample in order to achieve a critical excitation rate on the axis of the laser situated at a depth  $x$  below the surface

$$F^0 = \frac{hc}{\lambda_0 K(x)} R \quad (9)$$

where

$$K(x) = \int \exp[-\alpha(\lambda)x] \alpha(\lambda) d\lambda \quad (10)$$

In these equations  $\alpha$  is the absorption constant and  $\lambda_0$  is an average wavelength for the effective pump band, namely, the region of the absorption spectrum where the integrand of (10) has an appreciable value. Computations of the effective pump bands and thresholds for different sample geometries and chelate concentrations are given in Ref. 2. For samples of 0.1-cm diameter, the calculated threshold flux is about 2.5 watts/cm<sup>2</sup> per angstrom in the region of 3900 Å, whereas for ruby it is 1.3 watts/cm<sup>2</sup> per angstrom in the green absorption band. Since the flash lamps emit more in the blue range of the spectrum, the two thresholds should be quite comparable.

#### 4.2 Apparatus

The most important problem in the development of the chelate laser was the design of a suitable cavity to contain the liquid. The major difficulty encountered here is the large contraction of the liquid on cooling. The alcohol solution has a coefficient of expansion of 0.001 cm/cm per °C

so that a 20 percent linear contraction occurs on cooling to the operating temperature. This problem was solved by the use of piston cells described previously and shown in Fig. 12. When properly machined, the pistons will follow the contraction of the liquid in contact with the solution until, below  $-160^{\circ}\text{C}$ , the viscosity of alcohol becomes so large that the pistons tend to bind, and voids easily form in the still-contracting solution. To eliminate this possibility, the cells are usually operated at temperatures no lower than  $-150^{\circ}\text{C}$ . Low temperatures were achieved by passing a stream of pre-cooled nitrogen gas over the cells. In most experiments confocal mirrors 2 inches apart were used. For the excitation of the cells, various configurations of more or less conventional flash tubes and enclosures have been employed.<sup>4,31</sup> Because of the high absorption, the chelate lasers are effectively pumped only in the blue and near uv region of the spectrum. It is desirable to use a filter around the cells to eliminate as much as possible radiation that only contributes to heating.

#### 4.3 Output Power

With resonator cells of 1-mm bore, as shown in Fig. 12a, their small transverse dimension makes it possible to achieve high pumping rates on the axis of the cells. This results in easily interpretable laser phenomena. The original experiments with chelate lasers were performed in cells with 0.4-cm diameter, as shown in Fig. 12b; these structures give rise to a more complicated behavior to be described later.

The threshold for laser action is about 500 joules when a spiral GE524 flash lamp is used. This is about one-half of the threshold of a ruby crystal of 0.4-cm diameter and 5-cm long, placed in the same flash apparatus. Thus the cavity losses and the computation of threshold given above are seen to be approximately correct.

Measurements of the output energy were made with a calibrated photodiode (EG&G "Litemike"). The energy depends markedly on the transmittivity of the front mirror whose optimum value has been found to lie between 5 and 10 percent. The variation of output with electrical input is shown in Fig. 9. At 3000 joules the output reaches about 1 millijoule. Since the total volume

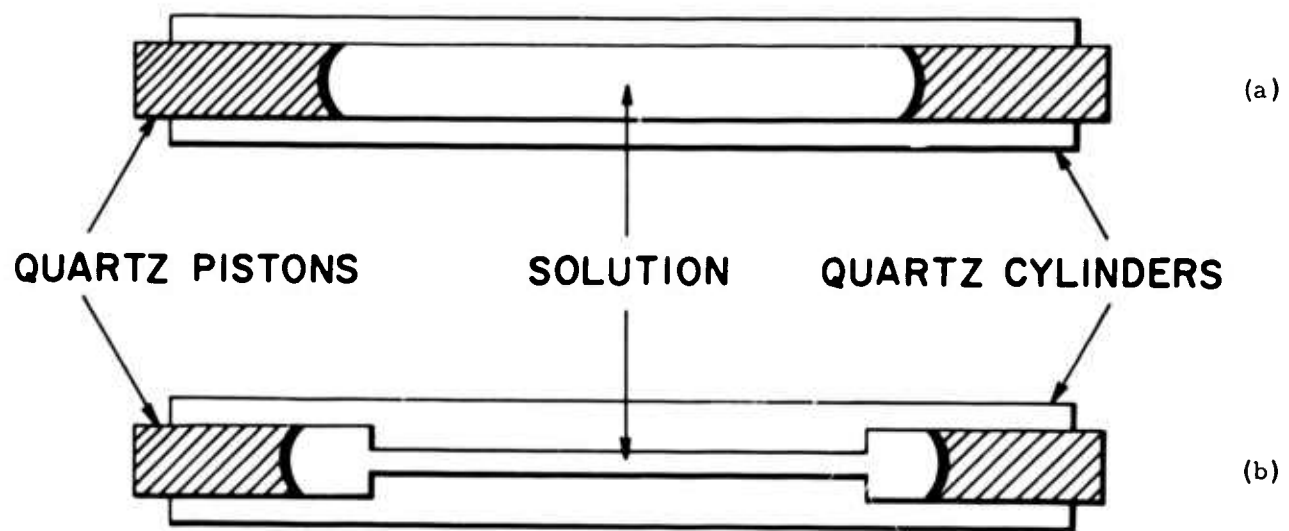


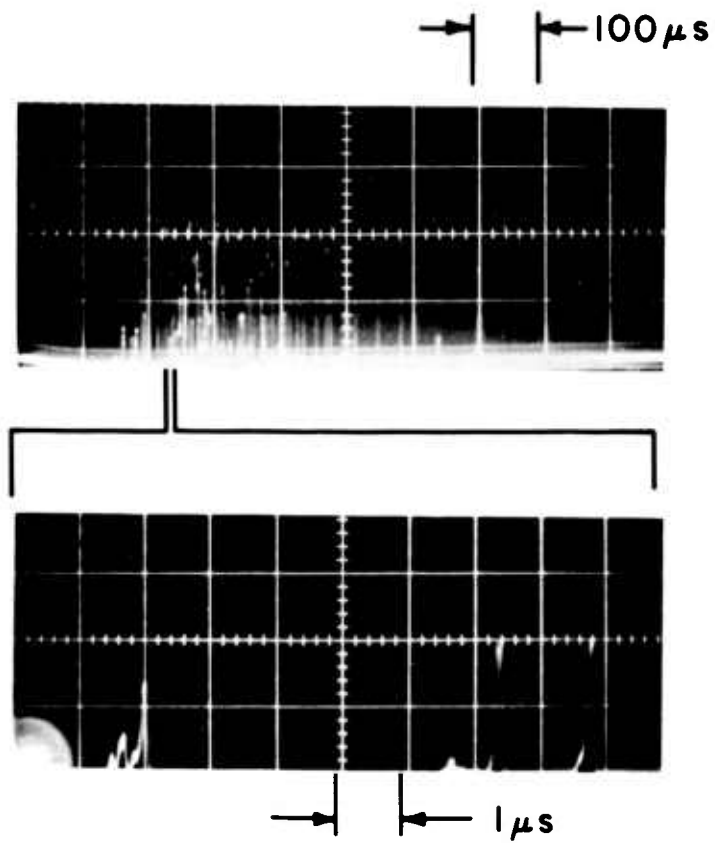
Fig. 12. Cells used in laser experiments (a) 1 mm bore, (b) 4 mm bore.

of the solution is  $0.03 \text{ cm}^3$ , the energy output is  $\sim 30 \text{ millijoule/cm}^3$ . This is the significant value to be used for comparison with other materials. For ordinary ruby crystals the energy per unit volume is about three to five times larger.<sup>32</sup> The time dependence of the output of the 1-mm cells is characterized by irregular spikes, very similar to those observed in ruby. A typical case is illustrated in Fig. 13.

#### 4.4 Output Beam Characteristics

The spectral output was analyzed by means of a Fabry-Perot interferometer. Below threshold no rings appear. Above threshold (Fig. 14), rings having a structure corresponding to the presence of several longitudinal modes are clearly visible. The width of the individual frequency components is below  $0.1 \text{ cm}^{-1}$ . Another type of structure is also evident. The rings have a spotty nature, each spot having a diameter ( $7 \times 10^{-4} \text{ rad}$ ) consistent with the diffraction pattern from a 1-mm aperture. The spots correspond therefore to discrete pencils of light representing off-axis modes. Close to threshold, the mode structure is sometimes much simpler. Figure 15 (a) is a near field photograph at threshold showing a single  $\text{TEM}_{01}$  transverse mode. At higher energies, the entire aperture of the laser is filled with a granular structure. This structure persists along the beam and can be detected by simply placing a film (without lens) anywhere along the path as shown on Fig. 15(b). Similar observations were made by Schimitschek.<sup>33</sup>

Quite different results are obtained when the large bore (4-mm) cells with confocal mirrors are used for laser experiments. In this case the thickness is much too large for any appreciable pumping to occur on the axis of the cells, and laser action is confined to an annulus close to the surface.<sup>4</sup> The relaxation no longer consists of random spikes but of a very regular undamped oscillation as shown in Fig. 16. This type of behavior has been associated with a saturable loss mechanism.<sup>34-36</sup> The near- and far-field patterns do not reveal any structure that can be identified as simple modes. The line width above threshold is somewhat broader ( $\sim 0.2 \text{ cm}^{-1}$ ) than in the 1-mm cavities, and usually shows no structure.



### SPHERICAL MIRRORS

Fig. 13. Relaxation oscillation (random spikes) obtained from  $\text{EuB}_4\text{P}$  in 1 mm cavity. Confocal mirrors,  $R = 2$  inches.

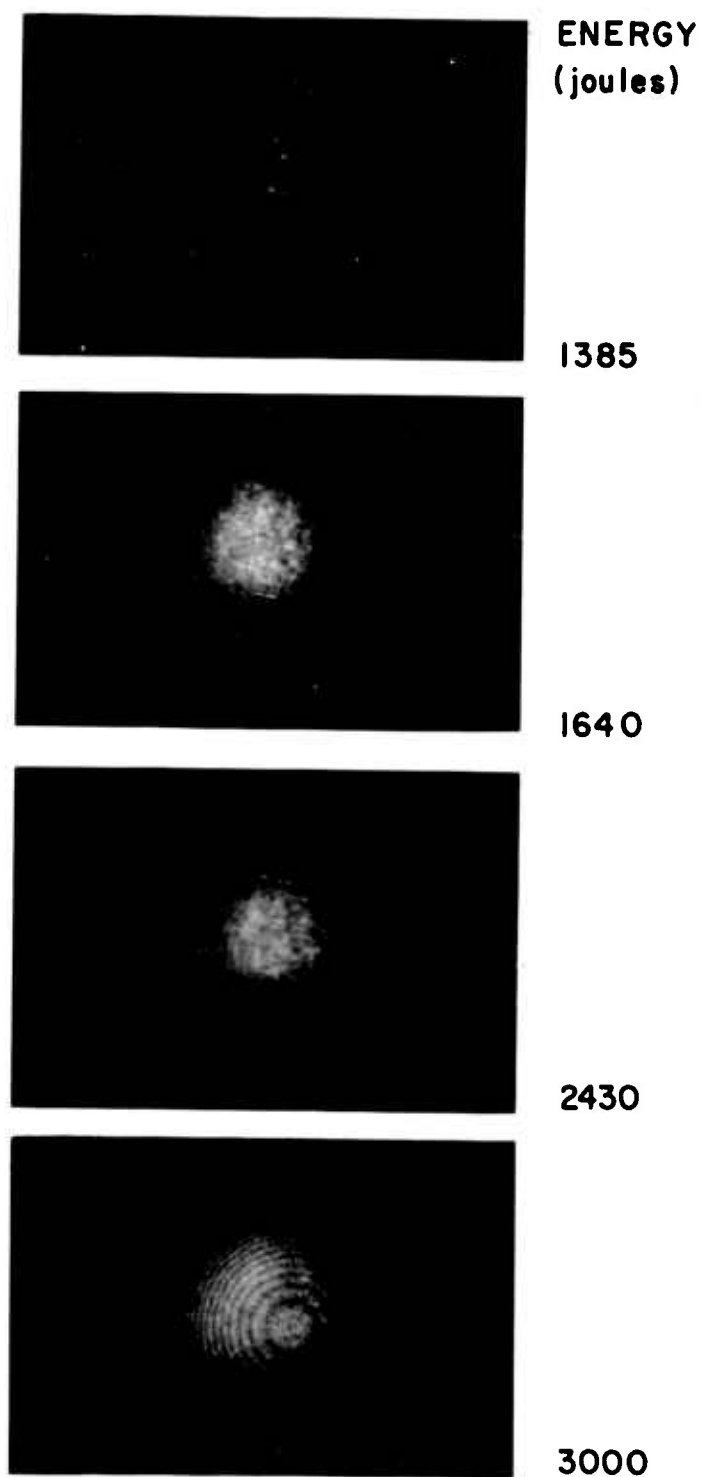


Fig. 14. Fabry-Perot interferograms of the output of  $\text{EuB}_4\text{P}$  in alcohol solution.

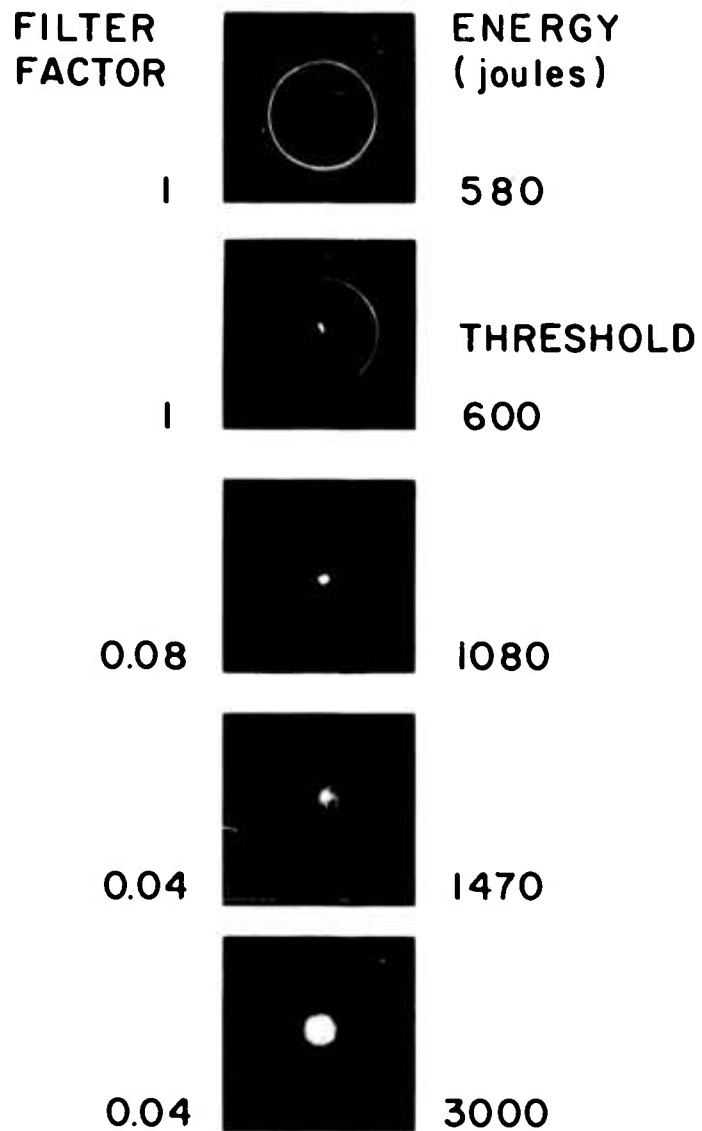


Fig. 15(a) Near-field pattern of laser emission from 1-mm cell obtained with camera focused on front mirror. Note appearance of single mode at threshold. The outer ring in the two top photographs is due to flash leakage around the 4-mm piston.

FILTER  
FACTOR

1.0



ENERGY  
(joules)

630

1.0



(THRESHOLD)

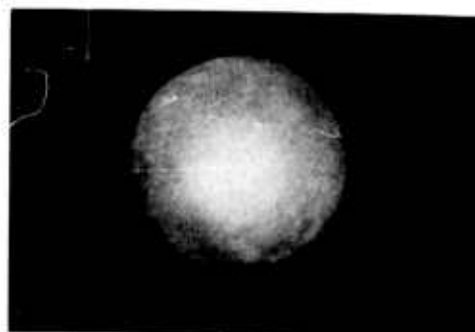
690

0.35



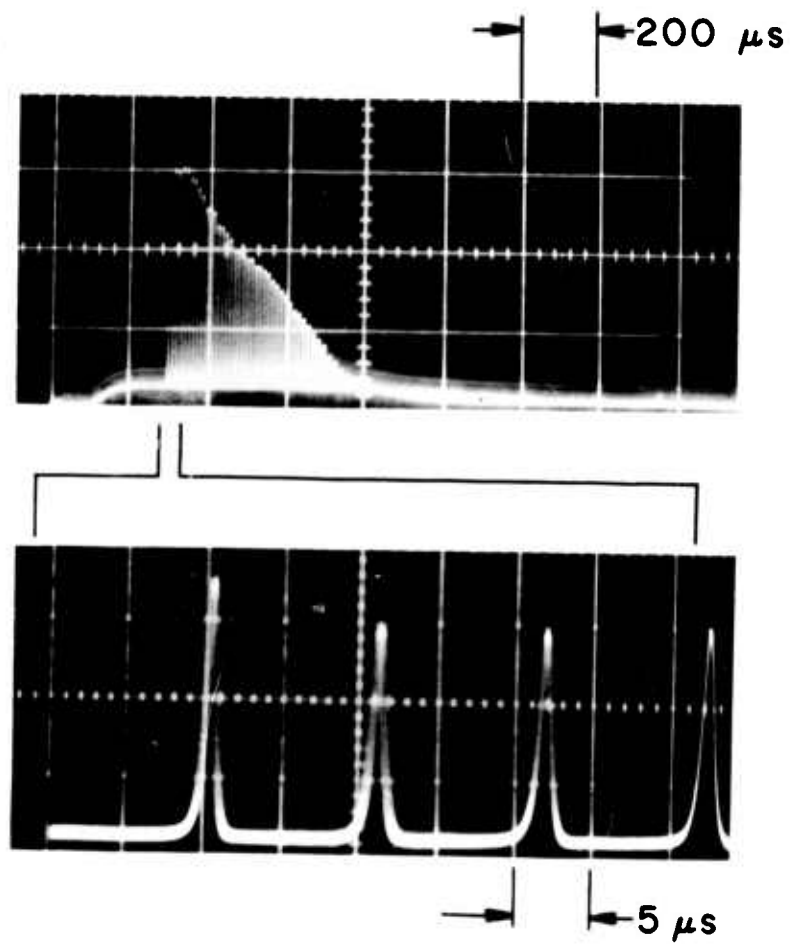
1080

0.002



3000

Fig. 15(b). Intermediate-field pattern of laser emission obtained on film placed 30 inches from laser (without lens).



**SPHERICAL MIRRORS**

Fig. 16. Regular relaxation pattern (limit cycle) characteristic of  $\text{EuB}_4\text{P}$  in large (4 mm) cells.

These phenomena, which have not been studied in great detail, are undoubtedly associated with the very high density of modes.

#### 4.5 Quality of the Optical Cavity

Insight into the losses can be obtained from a study of the dependence of threshold on the concentration, as shown in Fig. 17. As the concentrations are decreased the threshold changes relatively little, until a very rapid increase occurs when concentrations of the order of  $10^{18}$  per  $\text{cm}^3$  are reached. This is exactly what one would expect from the computation of the effective pump band. It is shown in Fig. 5 of Ref. 2 that the parameter  $K$  changes little with the concentration. When, however, the concentration approaches the minimum  $\Delta n$ , determined by the cavity losses, the threshold rises abruptly. Thus, knowing the minimum concentration, we can calculate the losses; these are of the order of 6 percent per pass, comparable with crystalline materials. The measurement of losses by determining the minimum lasing concentration is carried out quite easily in the liquid laser.

The losses in the cavity can also be determined by the method of Yariv and Gordon.<sup>37</sup> This consists in determining the output power at a fixed position of the pump energy above threshold for varying mirror transmissions. Such a series of measurements is shown graphically in Fig. 18. There exists an optimum ratio of mirror transmission to average loss per pass,  $S_{\text{opt}}$ , which, for a given input energy,  $E_{\text{in}}$  maximizes the energy output. This is given by:

$$S_{\text{opt}} = -1 + (E_{\text{in}}/E_{\text{min}})^{1/2}, \quad (11)$$

where  $E_{\text{min}}$  is the threshold energy. For the data in Fig. 18, the loss per pass is between 10 and 25 percent. Thus, on going from threshold input energy to twice this value, the loss increases by about a factor of 3. This is to be expected since the fluid medium is perturbed much more by the higher input energy.

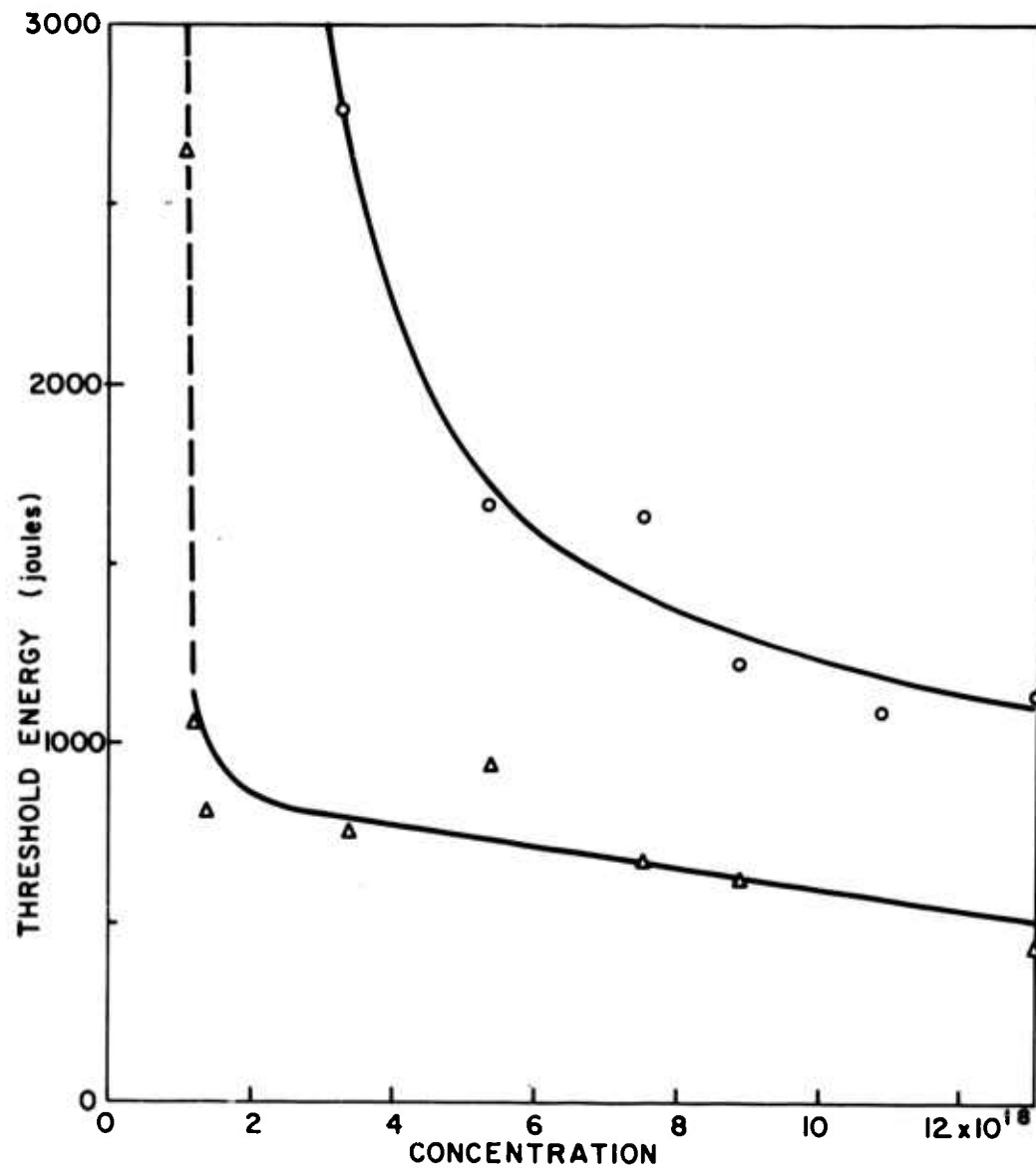


Fig. 17. Dependence of laser threshold of  $\text{EuB}_4\text{P}$  in alcohol solution on concentration. Dielectric mirror transmission:  $\circ$ -6.6%;  $\Delta$ -0.1%. Cell 0.1 cm diameter.

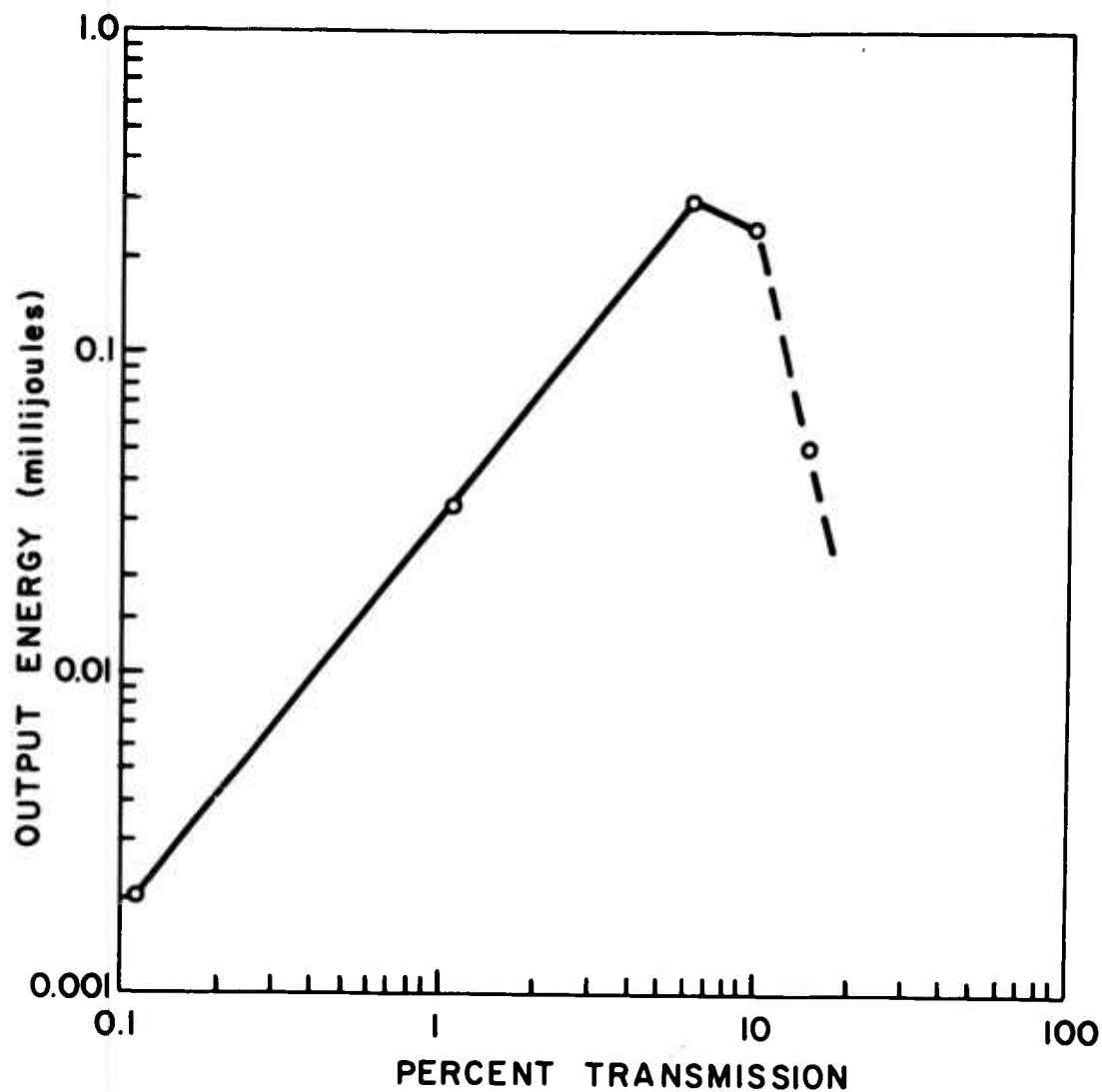


Fig. 18. Output energy of the 0.10-cm cell vs percent transmission of front mirror at twice threshold ( $E_{in}/E_{min} = 2$ ). Concentration:  $9 \times 10^{18} \text{ cm}^{-3}$ .

The behavior of a liquid cavity at higher temperatures and hence under more fluid conditions has not been determined. Nevertheless, losses cannot be too high since laser action has been observed under these conditions.

## 5. CONCLUSIONS AND FUTURE WORK

There are several important conclusions which can be formulated at this stage of the investigation of chelate systems:

1. Laser action can be obtained in a highly fluid medium at room temperature. This opens an entirely new technology since a laser with a circulating medium is now only a technological problem.
2. The study of the spectroscopy of chelates has revealed detailed information on the structure, symmetry and stability of various compounds. From the evidence known at present, it appears that 4-ligand materials are superior from the laser point of view.
3. The great flexibility of chelate systems, anticipated at the beginning of this work, has now been demonstrated by such effects as the "tuning" achieved by cation addition and the variety of solvent influences.

Each of these findings has raised new questions and each is, at best, only partially understood.

The dominant practical problem of excessive absorption is yet to be solved. It prevents the use of large samples and this keeps the useful power output at a low level. It is also responsible for the high thresholds that effectively eliminate the possibility of realizing the potential of continuous operation. Our past work has not been directly concerned with the details of energy transfer and its relation to structural factors, but it is hoped to devote more effort to these aspects in future studies.

PAPERS PUBLISHED IN 1964

1. Laser Action in Europium Chelates I: Spectroscopic Properties of Europium Benzoylacetate. *J. Chem. Phys.* 40, 2547 (1964). H. Samelson, A. Lempicki, V.A. Brophy and C. Brecher.
2. Laser Action in Europium Chelates II: Kinetics and Optical Pumping in Europium Benzoylacetate. *J. Chem. Phys.* 40, 2553 (1964). H. Samelson, A. Lempicki and C. Brecher.
3. Laser Action in Europium Chelates III: Spectroscopic Effects of Chemical Composition and Molecular Structure. *J. Chem. Phys.*, to be published. C. Brecher, H. Samelson and A. Lempicki.
4. Laser Action in Europium Chelates IV: Characteristics of the Europium Benzoylacetate Laser. *J. Chem. Phys.* 41, 1214 (1964). A. Lempicki, H. Samelson and C. Brecher.
5. Evidence for Eight-fold Coordination in Europium Chelates. *J. Chem. Phys.* 41, 279 (1964). C. Brecher, A. Lempicki and H. Samelson.
6. Room Temperature Operation of a Europium Chelate Liquid Laser. *App. Phys. Letters*, to be published. H. Samelson, A. Lempicki, C. Brecher and V. A. Brophy.
7. Shift in the Frequency of the Emission of the Europium Benzoylacetate Laser. *J. Chem. Phys.*, to be published. H. Samelson, V. A. Brophy, C. Brecher and A. Lempicki.
8. Chelates as Laser Materials. *Applied Optics*, to be published. A. Lempicki, H. Samelson and C. Brecher.
9. Stimulated Emission in Some Rare Earth Chelates. *Nature* 202, 580 (1964). C. Brecher, A. Lempicki and H. Samelson.
10. Europium Chelates as Laser Materials. *Proceedings IV Rare Earth Conference, Phoenix, Ariz., April 1964.* A. Lempicki, H. Samelson and C. Brecher.
11. *Proceedings of Conference on Organic Lasers. Held at GT&E Laboratories, Bayside, N. Y., May 25, 1964.* A. Lempicki and H. Samelson, Ed.

## REFERENCES

1. H. Samelson, A. Lempicki, V. A. Brophy and C. Brecher. *J. Chem. Phys.* 40, 2547 (1964).
2. H. Samelson, A. Lempicki and C. Brecher. *J. Chem. Phys.* 40, 2553 (1964).
3. C. Brecher, H. Samelson and A. Lempicki. *J. Chem. Phys.*, to be published.
4. A. Lempicki, H. Samelson and C. Brecher. *J. Chem. Phys.* 41, 1214 (1964).
5. C. Brecher, A. Lempicki and H. Samelson. *J. Chem. Phys.* 41, 279 (1964).
6. H. Samelson, A. Lempicki, C. Brecher and V. A. Brophy. *App. Phys. Letters*, to be published.
7. H. Samelson, V. A. Brophy, C. Brecher and A. Lempicki. *J. Chem. Phys.*, to be published.
8. S. I. Weissman. *J. Chem. Phys.* 10, 214 (1942).
9. G. A. Crosby, R. E. Whan, and R. M. Alire. *J. Chem. Phys.* 34, 743 (1961).
10. M. Metlay. *J. Chem. Phys.* 39, 491 (1963).
11. F. Halverson, J. S. Brinen and J. R. Leto. *J. Chem. Phys.* 41, 157 (1964).
12. R. Charles and A. Perrotto. *J. Inorg. Nuc. Chem.* 26, 273 (1964).
13. M. L. Bhaumik, P. C. Fletcher, S. Higa, S. M. Lee, L. J. Nugent, C. L. Telk, and M. Weinberg. *J. Phys. Chem.* 68, 1490 (1964).
14. L. C. Thompson, J. A. Loraas. *J. Inorg. Chem.* 2, 89 (1963).
15. J. L. Hoard, M. D. Lind, and B. K. Lee. Fourth Rare Earth Research Conference, Session III, April 1964.
16. G. F. Pope, J. F. Steinback and W. F. Wagner, *J. Inor. Nuc. Chem.* 20, 304 (1961).
17. A. Lempicki and H. Samelson. *Physics Letters* 4, 133 (1963).
18. R. E. Whan and G. A. Crosby. *J. Molec. Spectr.* 8, 315 (1962).

19. Staniforth and McReynolds. Thesis. Ohio State University.
20. A. E. Martell and M. Calvin. Chemistry of Metal Chelate Compounds, Prentice-Hall, N. Y. (1952).
21. A. Lempicki and H. Samelson. App. Phys. Letters 2, 159 (1964).
22. M. Kleinerman, Private Communication.
23. H. Winston. J. Chem. Phys. 39, 267 (1963).
24. N. E. Wolff and R. J. Pressley. App. Phys. Letters 2, 152 (1963).
25. H. Samelson and A. Lempicki. J. Chem. Phys. 39, 110 (1963).
26. C. Brecher, A. Lempicki and H. Samelson. J. Chem. Phys. 41, 279 (1964).
27. Y. Meyer, H. Poncet, and M. Verron. Comptes Rendus Acad. Sc. Paris 259, 103 (1964).
28. E. J. Schimitschek reports laser action with Eu(TTA)<sub>3</sub>P in this solvent at -20 to -30°C. Chemical Laser Conference, <sup>4</sup>La Jolla, Calif., Sept. 1964.
29. A. L. Schawlow and C. H. Townes. Phys. Rev. 112, 1940 (1958).
30. H. Winston and R. A. Gudmundsen. Applied Optics 3, 143 (1964).
31. A. Lempicki and H. Samelson. Proceedings of Symposium on Optical Masers, Polytechnic Press, Brooklyn, N. Y., p. 347 (1963).
32. T. Li and S. D. Sims. Applied Optics 1, 325 (1962).
33. E. J. Schimitschek. App. Phys. Letters 3, 117 (1963).
34. E. Snitzer. Quantum Electronics, Proc. of the Third International Congress, Paris. Columbia Univ. Press, Vol. II, p. 999 (1964).
35. W. R. Sooy, R. S. Congleton, B. E. Dobratz and W. K. Ng Ibid., Vol. II, p. 1103.
36. K. Shimoda. Proceedings of the Symposium on Optical Masers, Polytechnic Press, Brooklyn, N. Y., p. 95 (1963).
37. A. Yariv. Proc. IEEE 51, 1723 (1963).

NOmr-4134(00) .

DISTRIBUTION LIST

R. S. Congleton  
Hughes Aircraft Corp.  
Aerospace Group  
Research & Development Division  
Culver City, California

Basil Curnutte, Jr.  
Kansas State University  
Manhattan, Kansas

G. H. Dieke  
Johns Hopkins University  
Baltimore 18, Maryland

C. H. Keller  
Pek Labs. Inc.  
925 Evelyn Avenue  
Sunnyvale, California

S. P. Keller  
International Business Machines  
T. J. Watson Research Center  
Yorktown Heights, New York

A. Lempicki  
General Telephone & Electronics  
Bayside 60, New York

R. C. Pastor  
Korad Corporation  
2520 Colorado Avenue  
Santa Monica, California

T. C. McAvoy  
Corning Glass Works  
Corning, New York

W. McKusick  
Eastman Kodak Company  
Apparatus and Optical Division  
400 Plymouth Avenue, N.  
Rochester 4, New York

O. H. Nestor  
Linde Company  
1500 Polco Street  
Indianapolis 24, Indiana

J. W. Nielson  
Airtron, A Div. of Litton Industries  
200 East Hanover Avenue  
Morris Plains, New Jersey

Gerald Oster  
Chemistry Department  
Polytechnic Institute of Brooklyn  
333 Jay Street  
Brooklyn 1, New York

David Stockman  
Electronics Laboratory  
General Electric Company  
Syracuse, New York

J. W. Turner  
Westinghouse Electric Corp.  
Electronics Division  
P. O. Box 1897  
Baltimore 3, Maryland

R. W. Young  
American Optical Company  
Southbridge, Massachusetts

Dr. Jerald R. Izatt  
New Mexico State University  
University Park, New Mexico

Professor A. K. Kamal  
Purdue University  
School of Electrical Engineering  
Lafayette, Indiana

Mr. Thomas C. Marshall  
Columbia University  
Dept. of Electrical Engineering  
New York 27, New York

Mr. Charles G. Naiman  
Mithras, Inc.  
Cambridge 39, Massachusetts

---

One copy each unless otherwise specified.

Dr. J. H. Schulman  
Solid State Division  
U. S. Naval Research Laboratory  
Washington 25, D.C.

Bureau of Naval Weapons /RR-2/  
Department of the Navy  
Washington 25, D. C.  
ATTN: Dr. C. H. Harry

Dr. Jack A. Soules  
Physics Department  
New Mexico State University  
University Park, New Mexico

Bureau of Ships /Code 305/  
Department of the Navy  
Washington 25, D.C.  
ATTN: Dr. G. C. Sponsler

Dr. Arden Sher  
Varian Associates  
611 Hansen Way  
Palo Alto, California

Office of Naval Research  
Department of the Navy  
Washington 25, D. C.  
ATTN: Dr. Sidney Reed

Physical Sciences Division  
Army Research Office  
Office, Chief, Research & Develop.  
Washington 25, D. C.  
ATTN: Dr. Robert A. Watson

Office of Naval Research  
Department of the Navy  
Washington 25, D. C.  
ATTN: Mr. Frank B. Isakson (3 copies)

Chief Scientist  
U. S. Army Electronics Command  
Fort Monmouth, New Jersey  
ATTN: Dr. Hans K. Ziegler

Office of Naval Research  
Department of the Navy  
Washington 25, D. C.  
ATTN: Mr. J. W. Smith

Director, Inst. for Explatory Res.  
Army Signal Research &  
Development Laboratory  
Fort Monmouth, New Jersey  
ATTN: Dr. E. M. Reilley

Naval Research Laboratory  
Department of the Navy  
Washington 25, D. C.  
ATTN: Dr. C. C. Klick

Asst. Director of Surveillance  
Army Signal Research and  
Development Laboratory  
Fort Monmouth, New Jersey  
ATTN: Dr. Harrison J. Merrill

Naval Research Laboratory  
Department of the Navy  
Washington 25, D. C.  
ATTN: Dr. L. F. Drummeter

Director of Research & Development  
Army Ordnance Missile Command  
Huntsville, Alabama  
ATTN: Mr. William D. McKnight

Headquarters USAF /AFRDR-NU-3/  
Department of the Air Force  
Washington, D. C.  
ATTN: Lt. Col. E. N. Myers

Office, Chief of Naval Operations  
Department of the Navy  
Washington 25, D. C.  
ATTN: Mr. Ben Rosenberg

Research & Technology Division  
Bolling AFB  
Washington, D. C.  
ATTN: Mr. Robert Feik

Office, Aerospace Research /MROSP/  
Washington 25, D. C.  
ATTN: Lt. Col. Ivan Atkinson

One copy each unless otherwise specified.

Technical Area Manager /760A/  
Advanced Weapons Aeronautical  
Systems Division  
Wright-Patterson AFB  
Ohio  
ATTN: Mr. Don Newman

Project Engineer /5237/  
Aerospace Radiation Weapons  
Aeronautical Systems Division  
Wright-Patterson AFB  
OHIO  
ATTN: Mr. Don Lewis

Air Force Special Weapons Center  
Kirtland AFB  
New Mexico  
ATTN: Capt. Marvin Atkins

Project Engineer /5561/ Comet  
Rome Air Development Center  
Griffiss AFB  
New York  
ATTN: Mr. Phillip Sandler

Department of Electrical Engineering  
New York University  
University Heights  
New York, New York  
ATTN: Mr. Thomas Henion

BMDR  
Room 2 B 263  
The Pentagon  
Washington 25, D.C.  
ATTN: Lt. Col. W.B. Lindsay (8 copies)

Mr. John Emmett  
Physics Department  
Stanford University  
Palo Alto, Calif.

Secretary, Special Group Optical Masers  
ODDRCE Advisory Group Electron Devices  
346 Broadway - 8th Floor  
New York 13, New York (3 copies)

ASD /ASRCE - 31/  
Wright-Patterson AFB  
Ohio

Dr. W. Holloway  
Sperry Rand Research Center  
Sudbury, Massachusetts

Technical Area Manager /760B/  
Surveillance Electronic Systems Div.  
L. G. Hanscom AFB  
Massachusetts  
ATTN: Major H. I. Jones, Jr.

Commanding Officer  
U. S. Naval Ordnance Laboratory  
Corona, Calif.

Director  
U.S. Army Engineering Research  
and Development Laboratories  
Fort Belvoir, Virginia  
ATTN: Technical Documents Center

Office of the Director of Defense  
Defense Research and Engineering  
Information Office Library Branch  
Pentagon Building  
Washington 25, D. C. (2 copies)

U. S. Army Research Office  
Box CM, Duke Station  
Durham, North Carolina (2 copies)

Defense Documentation Center  
Cameron Station Building  
Alexandria 14, Virginia (20 copies)

One copy each unless otherwise specified.

Director U. S. Naval Research Laboratory Technical Information Officer Code 2021 Washington 25, D. C. ( 6 copies)	Commanding Officer U.S. Army Materials Research Agency ATTN: Technical Library Watertown, Massachusetts 02172
Commanding Officer Office of Naval Research Br. Office 230 N. Michigan Avenue Chicago, Illinois 60601	Boulder Laboratories National Bureau of Standards ATTN: Library Boulder, Colorado
Commanding Officer Office of Naval Research Br. Office 207 W. 44th Street New York , New York 10011	Air Force Weapons Laboratory ATTN: Guenther WLRPF Kirtland Air Force Base New Mexico
Commanding Officer Office of Naval Research Br. Office 1000 Geary Street San Francisco, California 94109	Chief, Bureau of Naval Weapons Department of the Navy Washington 25, D. C. ATTN: J. M. Lee RMGA-81
Air Force Office of Scientific Res. Washington 25, D. C.	Air Force Cambridge Res. Lab. ATTN: CRXL-R, Research Library Lawrence G. Hanscom Field Bedford, Massachusetts
Director National Bureau of Standards Washington 25, D. C.	Battelle Memorial Institute 505 King Avenue Columbus 1, Ohio ATTN: BMI-Defender
Director Research Department U. S. Naval Ordnance Laboratory White Oak, Silver Spring, Md.	Headquarters, USAELRDL Fort Monmouth, New Jersey 07703 ATTN: SELRA/SAR, NO-4, X, and PF
Commanding Officer Office of Naval Research Br. Office 1030 East Green Street Pasadena, California 91101	Comm. U.S. Naval Ordn. Test Station China Lake, Calif. ATTN: Mr. G.A. Wilkins /Code 4041/
Commanding Officer Office of Naval Research Br. Office 495 Summer Street Boston 10, Mass.	J. C. Almasi General Electric Company Advanced Technology Laboratories Schenectady, N. Y.
U.S. Naval Radiological Defense Lab. /Code 941/ San Francisco, California 94135	Prof. Rubin Braunstein University of California Department of Physics Los Angeles 24, Calif.

One copy each unless otherwise specified.

N. I. Adams  
Perkin-Elmer Corp.  
Norwalk, Conn.

E. P. Reidel  
Quantum Electronics Dept.  
Westinghouse Electric Corp.  
Research Laboratories  
Pittsburgh, Pa.

Prof. H. G. Hanson  
University of Minnesota  
Duluth, Minn.

P. Schaffer  
Lexington Laboratories, Inc.  
84 Sherman Street  
Cambridge, Mass.

L. E. Rautiola  
Linde Company  
Div. of Union Carbide  
East Chicago, Ind.

F. S. Galasso  
United Aircraft Corp.  
Research Labs.  
400 Main Street  
East Hartford, Conn.

J. W. Nielson  
Airtron, Division of  
Litton Industries  
Morris Plains, N. J.

E. M. Flanigen  
Linde Company  
Division of Union Carbide  
Tonawanda, New York

W. Prindle  
American Optical Company  
14 Mechanic Street  
Southbridge, Mass.

R. G. Meyerland  
Plasma Physics  
United Aircraft Corp.  
East Hartford 8, Conn.

Prof. N. Bloembergen  
Harvard University  
Div. of Engineering and  
Applied Physics  
Cambridge 38, Mass.

Prof. R. J. Collins  
University of Minnesota  
Department of Electrical Eng.  
Minneapolis 14, Minn.

Dr. Alan Kolb  
U. S. Naval Research Lab.  
Washington, D. C.

Prof. J. M. Feldman  
Carnegie Institute of Technology  
Department of Electrical Engr.  
Pittsburgh 13, Penna.

Prof. Arthur Schawlow  
Stanford University  
Stanford, California

Research Materials Information Center  
Oak Ridge National Laboratory  
Post Office Box X  
Oak Ridge, Tenn. 37831

J-5 Plans and Policy Directorate  
Joint Chiefs of Staff  
Requirements and Develop. Div.  
ATTN: Special Projects Branch  
Room 2D982, The Pentagon  
Washington, D. C., 20301

Advanced Research Projects Agency  
Research and Development Field Unit  
APO 143, Box 41  
San Francisco, Calif.

---

One copy each unless otherwise specified.

Advanced Research Projects Agency  
Research & Development Field Unit  
APO 146, Box 271  
San Francisco, California  
ATTN: Mr. Tom Brundage

Air Force Materials Laboratory  
Air Force Systems Command  
Wright-Patterson AFB, Ohio 45433  
ATTN: MAAM (Lt. John H. Estess)

Dr. C. H. Church  
Westinghouse Electric Corporation  
Research Laboratories  
Pittsburgh 35, Penna.

Prof. Donald S. McClure  
Institute for the Study of Metals  
University of Chicago  
Chicago 37, Illinois

Dr. Daniel Grafstein  
General Precision, Inc.  
Aerospace Group  
Little Falls, New Jersey

Professor R. C. Ohlmann  
Westinghouse Research Lab.  
Pittsburgh, Penna.

Dr. R. C. Linares  
Perkin-Elmer Corporation  
Solid State Materials Branch  
Norwalk, Connecticut 06852

Dr. J. G. Atwood  
Perkin-Elmer Corporation  
Electro-Optical Division  
Norwalk, Connecticut

Professor S. Claesson  
Uppsala University  
Uppsala, Sweden

---

One copy each unless otherwise specified.

**UNCLASSIFIED**

**UNCLASSIFIED**